UNIVERSIDAD REGIONAL AMAZÓNICA IKIAM
Facultad de Ciencias de la Tierra y Agua

Carrera de Hidrología.

Uso de SIG y R para estimar los impactos del cambio climático en la recarga de agua subterránea en la cuenca del río Portoviejo, Ecuador.

Autor: Angel Steven Intriago Mendoza.
Tutor: Bruno Pirilo Conicelli.

Tena, enero 2022
Napo, Ecuador

Declaración de derecho de autor, autenticidad y responsabilidad

Tena, 20 de septiembre de 2021

Yo, Angel Steven Intriago Mendoza con documento de identidad N° 1316350279, declaro que los resultados obtenidos en la investigación que presento en este documento final, previo a la obtención del título Ingeniero en Ciencias del Agua, son absolutamente inéditos, originales, auténticos y personales.

En virtud de lo cual, el contenido, criterios, opiniones, resultados, análisis, interpretaciones, conclusiones, recomendaciones y todos los demás aspectos vertidos en la presente investigación son de mi autoría y de mi absoluta responsabilidad.

Por la favorable atención a la presente, suscribo de usted,

Atentamente,

Firma:



_____

Angel Steven Intriago Mendoza
1316350279

INVESTIGACIÓN | Parroquia Muyuna, kilómetro 7 vía a Alto Tena
INNOVACIÓN | Tena · Napo · Ecuador
EDUCACIÓN | Telf.: (06) 370 0040 · (06) 299 9160
www.ikiam.edu.ec
@u_ikiam IkiamOficial u_ikiam Universidad Ikiam

Certificado de dirección de trabajo de integración curricular

Certifico que el trabajo de integración curricular titulado: “Uso de SIG y R para estimar los impactos del cambio climático en la recarga de agua subterránea en la cuenca del río Portoviejo, Ecuador”, en la modalidad de proyecto de investigación en formato artículo original, fue realizado por: Angel Steven Intriago Mendoza, bajo mi dirección.

El mismo ha sido revisado en su totalidad y analizado por la herramienta de verificación de similitud de contenido; por lo tanto, cumple con los requisitos teóricos, científicos, técnicos, metodológicos y legales establecidos por la Universidad Regional Amazónica Ikiam, para su entrega y defensa.

Tena, 20 de septiembre de 2021

Firma:

Firmado electrónicamente por:
BRUNO PIRILO

Bruno Pirilo Conicelli
C.I: 1759149774
Tutor

INVESTIGACIÓN | Parroquia Muyuna, kilómetro 7 vía a Alto Tena
INNOVACIÓN | Tena · Napo · Ecuador
EDUCACIÓN | Telf.: (06) 370 0040 · (06) 299 9160
www.ikiam.edu.ec
@u_ikiam IkiamOficial u_ikiam Universidad Ikiam

Agradecimientos.

Agradezco a mis padres por hacer posible cada paso que me ha llevado hasta aquí, por acompañarme, por siempre creer en mí, por el apoyo incondicional en todo sentido, por todo lo bueno y malo.

A mis profesores, especialmente a mi tutor de tesis, que han dado lo mejor de sus vidas para que un sueño como Ikiam sea posible, muchos de ellos con la única ambición de compartir su conocimiento. Gracias, por hacerme ver que la educación académica solo es un complemento prescindible en el proceso de mejora continua como persona.

A mis familiares, quienes han apoyado en los momentos más adversos de la familia. Cuando eres el mayor de tu generación, los que vienen detrás siempre serán una motivación para dar lo mejor de ti.

A mis compañeros de esta etapa universitaria, por su apoyo y ser como una segunda familia, siempre los tendré presente.

Al Ministerio de Ambiente, Agua y Transición Ecológica, por haber compartido sus proyecciones climáticas bajos los escenarios de cambio climático para el país; todo esto para poder desarrollar el presente tema de tesis.

Dedicatoria.

A la mujer que me enseñó mis primeras letras y números, mi abuela materna. No puedo dejar de preguntarme cual sería tu opinión al verme en esta etapa, luchaste hasta el final por verme crecer, lamentablemente no pudiste ganarle la batalla al cáncer. Me enseñaste a tener una actitud siempre positiva ante la vida; a dar batalla hasta el final, aunque esté todo perdido; a encontrar en el servicio a los demás un estilo de vida. Si estás en algún lugar, fuera de mis pensamientos, te lo dedico a ti.

Índice general.

1.- Introducción. 1

2.- Descripción del sitio. 2

3. Materiales y métodos. 4

3.1 Generación del mapa de escorrentía. 5

3.1.1.- Mapa de permeabilidad del suelo. 5

3.1.2.- Mapa de cobertura vegetal. 6

3.1.3.- Mapa de pendientes 7

3.1.4.Mapa de escorrentía superficial. 7

3.2.- Cálculo del balance hídrico. 8

3.2.1.- Precipitación. 9

3.2.2.- Temperatura. 10

3.2.3.- Evapotranspiración potencial. 11

3.2.4.- Escorrentía superfial. 12

3.2.5.- Agua retenida en el suelo 12

3.2.6. Agua retenida en el suelo menos evapotranspiración potencial. 12

3.2.7. Pérdida de agua acumulada 12

3.2.8.- Capacidad de campo. 12

3.2.9.- Cambios en la capacidad de campo. 14

3.2.10.- Déficit de agua. 14

3.2.11.- Evapotranspiración real. 14

3.2.12.- Percolación. 14

3.3.- Recarga de agua subterránea para los siguientes cincuenta años 14

4.- Resultados and discusión. 14

4.1.- Mapa de escorrentía resultante. 14

4.1.1.- Permeabilidad de suelo..... 15

4.1.2.- Capacidad de infiltración por uso de suelo..... 15

4.1.3.- Pendiente del terreno..... 15

4.1.4.- Integración de variables de entrada. 15

4.2.- Balances hídricos anuales. 16

4.3.- Recarga de agua subterránea actual..... 17

4.4.- Promedios de recarga de agua subterránea por décadas. 18

5. Conclusiones..... 23

Referencias..... 24

Índice de tablas.

Table 1.- Criterios para asignar coeficientes de escorrentía para cada clase. 8

Table 2.- Valores de la duración mensual media de la duración solarht corregidas y expresadas en periodos unidades de periodos de 12 horas (N) 12

Table 3.- Capacidad de campo (mm) de acuerdo al uso y tipo de suelo, adaptado de Thornthwaite y Mather (1957)..... 13

Índice de figuras.

Figura 1- Localización de la cuenca del río Portoviejo. 3

Figura 2.- Esquema metodológico del presente estudio. 5

Figura 3.- Reclasificación del mapa pedológico (izquierda) en dos clases (derecha). 6

Figura 4.- Reclasificación del mapa de uso de suelo (izquierda) en dos clases (derecha). 6

Figura 5.- Reclasificación del modelo digital de elevaciones (izquierda) de la cuenca del río Portoviejo en tres intervalos de pendientes (derecha).. 7

Figura 6.- Distribución espacial del coeficiente de escorrentía. 8

Figura 7.- Promedio anual pronosticado de precipitación y temperatura para la cuenca del río Portoviejo asumiendo un forzamiento radiativo de 4.5 W/m^2..... 10

Figura 8.- Promedio anual pronosticado de precipitación y temperatura para la cuenca del río Portoviejo asumiendo un forzamiento radiativo de 8.5 W/m^2..... 10

Figura 9.- Estimación de la distribución espacial de la capacidad del campo..... 13

Figura 10.- Balances hídricos desde 2021 hasta 2070 (RCP 4.5)..... 17

Figura 11.- Balances hídricos desde 2021 hasta 2070 (RCP 8.5)..... 17

Figura 12.- Recarga promedio desde 1985 hasta 2005..... 18

Figura 13.- Recarga de agua subterránea por décadas bajo el escenario RCP 4.5. 20

Figura 14.- Recarga de agua subterránea por décadas bajo el escenario RCP 8.5 22

Resumen.

Estimar la recarga futura de agua subterránea es fundamental para la gestión de recursos hídricos. Sin embargo, no existe información sobre esta en la cuenca del río Portoviejo (CRP), una zona semiárida con déficit hídrico donde los impactos del cambio climático podrían incrementar la presión sobre el agua subterránea. Debido a la simplicidad en las variables de entrada de entrada y exactitud en resultados, se utilizaron Sistemas de Información Geográfica para estimar la recarga de agua subterránea actual y futura (2021 – 2070) mediante balances hídricos, en la CRP. El estudio fue dividido en dos etapas. Primero, se obtuvo un mapa de escorrentía con las siguientes variables de entrada: permeabilidad del suelo, uso de la tierra y pendiente del terreno. En la segunda etapa, se obtuvo la recarga de agua subterránea usando la metodología de Thornthwaite y Mather. Los datos de precipitación y temperatura se consiguieron a partir de ensembles, obtenidos de modelos climáticos globales (MCG), los cuales usan dos escenarios de cambio climático (RCP 4.5 y RCP 8.5). Los resultados mostraron que la variabilidad en la precipitación y temperatura podría afectar la localización de zonas de recarga de agua subterránea para los siguientes cincuenta años. Actualmente, las tasas más altas de recarga (> 100 mm/año) están en las zonas rurales del cantón Portoviejo. Los futuros escenarios de recarga de agua subterránea proveen información para los tomadores de decisiones, debido a que las futuras zonas de recarga estarán localizadas en áreas de expansión de la ciudad de Portoviejo.

Palabras clave: Acuífero, SIG, cambio climático, recarga de agua subterránea, software libre.

Abstract.

Future groundwater recharge estimations are helpful tools for water resources management. However, there is a lack of information about that in many parts of the world, including the Portoviejo River watershed (PRW), a semi-arid zone with a water deficit where impacts of climate change could increase pressure on groundwater resources. Due to inputs simplicity and outputs accuracy, Geographical Information Systems were used to estimate current and future (2021 - 2070) groundwater recharge in PRW. This study was divided into two stages. First, a runoff map was obtained with the following input data: soil permeability, land use, and terrain slope. Second, current and future recharge were obtained through Thornthwaite and Mather water balances method. The input used were precipitation and temperature future data from two downscaled ensembles of four Global Climate Models, using representative concentration pathways (RCP) 4.5 and 8.5, and runoff spatial distribution. Results showed that future variability in precipitation and temperature would affect groundwater recharge zones for the next fifty years in both scenarios. The current scenario showed higher recharge rate zones (> 100 mm/year) in Portoviejo rural zones. In contrast, for the decade 2060-2070 and the scenario RCP 4.5, higher recharge rate zones are located around the current city of Portoviejo (urban zones) in the lowlands of the watershed. On the other hand, recharge rate areas increase considerably in the scenario RCP 8.5. Future groundwater recharge scenarios provide information to decision-makers about land use since future groundwater recharge zones will be located in expansion areas of Portoviejo city.

Keywords: Aquifer, GIS, climate change, groundwater recharge, open-source software.

Uso de SIG y R para estimar los impactos del cambio climático en la recarga de agua subterránea en la cuenca del río Portoviejo, Ecuador.

1.- Introduction.

Groundwater plays a significant role in rural zones of the Ecuadorian coast (Carrión et al., 2018). The location of groundwater recharge zones is essential for the integral management and sustainable use of groundwater (Saiz-Rodríguez et al., 2019); in semi-arid zones (Ehtiat et al., 2018), as the Portoviejo River watershed (PRW). Crucial parameters that determine the location of groundwater recharge zones are soil permeability (Thapa et al., 2017), land cover (Zomlot et al., 2017), slope terrain (Rukundo & Doğan, 2019), precipitation (Magesh et al., 2012), evapotranspiration (Rukundo & Doğan, 2019). Most of these parameters will be affected in the near future due to climate change.

Groundwater resources can have a nonlinear response to atmospheric conditions related to climate change (Holger et al., 2012). Therefore, impacts on groundwater recharge are expected to be higher than other water cycle stages. For example, in Brazil, relative changes in groundwater recharge (spanning −100% to +100%) are higher than relative changes in river flow (spanning -20% to 40%) (Hirata & Conicelli, 2012). Another example from Texas, suggest that future changes in average groundwater recharge (spanning −75% to +35%) will exceed the range estimated for future precipitation (spanning −25% to +20%) (Ng et al., 2010). Methodologies to estimate the impacts of climate change on groundwater recharge have used techniques such as soil water balance (Guevara-Ochoa et al., 2020), empirical models (Chen et al., 2002), conceptual models (Thampi & Raneesh, 2011), and Geographical Information Systems (GIS) (Hirata & Conicelli, 2012).

Although none of the techniques previously described is uncertainty free (Scanlon et al., 2002; Holman, 2006), GIS could provide useful information about the spatial distribution of groundwater recharge and availability (Conicelli et al., 2021; Boufekane et al., 2020; Yeh et al., 2016; Tilahun and Merkel, 2009; Singh et al., 2013).

A GIS-based index is a simplified representation of a system, which can increase its understanding. For example, each parameter can be weighted according to the characteristics that influence a determined process; several researchers have used different criteria for delineating groundwater recharge zones (Saiz-Rodríguez et al., 2019) (Chowdhury et al., 2010) (Senanayake et al., 2016). On the other hand, R open-source language programming has been used to develop a lumped model that estimates groundwater level time series at observation boreholes by linking algorithms to simulate soil drainage (Jackson, 2012). Also, a specific package to model the groundwater system of the Wood River Valley was developed in R (Fisher et al., 2016). However, there is no report of a

distributed model to calculate groundwater recharge, which combines the advantages of R and an open-source GIS software like QGIS.

The PRW is located in a semi-arid zone of the Ecuadorian coast, precisely in the Manabí province´s center-south. The watershed has 45% of rural households that depend on wells (National Institute of Statistics and Censuses (INEC), 2010). The largest urban center situated inside PRW is the city of Portoviejo. This medium urban center with expected fast growth in the following years, will lie over possible groundwater recharge zones. Identifying these zones is vital to protect groundwater resources from contamination, make possible the sustainable use of groundwater resources, and improve the resilience of the watershed to climate change. Thus, this paper aims to estimate current and future (2021 – 2070) groundwater recharge, combining a GIS-based distributed model and a water balance model programmed in R in the PRW. The analysis uses soil texture, land cover, and slope terrain to obtain the surface-runoff-coefficient spatial distribution. The water balance was developed using the Thornthwaite and Mather method. Information from downscaled ensembles of four global general circulation models (GCM) were used as precipitation and temperature inputs derived from two RCP´s.

2.- Site description.

The PRW is a hydrographic unit with around 2000 km^2, which includes mainly four cantons of the Manabí province: Portoviejo, Santa Ana, Rocafuerte, and 24th of May (Figure 1). PRW has a population of around 300,000 inhabitants, where superficial water is the primary water source for use inside homes. However, groundwater resources are indispensable for agriculture and human consumption in rural zones (National Institute of Statistics and Censuses (INEC), 2010).

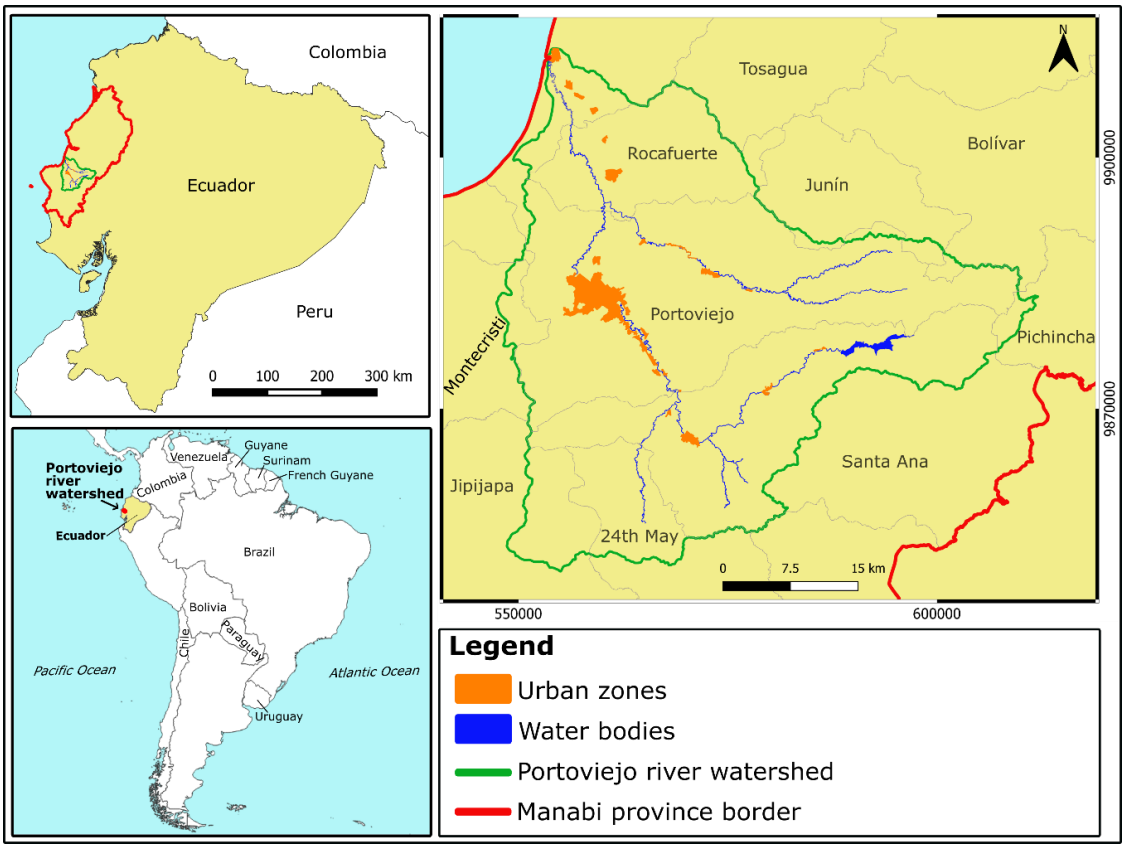


Figure 1- Location of Portoviejo River watershed.

The region has two well-defined seasons, a hot rainy season from December to April and a cold dry season between May and November (Thielen et al., 2016). Thus, the climate in the region is defined as warm, sub-humid, with a water deficit in the dry season (Giler-Ormaza, 2018). To face the water deficit, PRW imports water from more humid regions using a set of interconnected dams, collectively known as the Manabí Hydrological System (MHS), which was built more than 50 years ago (CRM et al., 1991). However, since its construction, MHS has been poorly maintained, which will likely compromise the water supply in the region, causing a possible increment of pressure on groundwater resources.

High values of Total Dissolved Solids (TDS) have been reported in groundwater resources. This poor groundwater quality could be related to the evaporation of rainfall, irrigation return flow, long residence times of water causing the dissolution of minerals, or marine intrusion into the groundwater system (Taheri & Voudouris, 2007). However, in the absence of information related to recharge zones, and the answer is yet to be found.

About the hydrogeology, inside PRW is located the Charapoto-Portoviejo-Riochico aquifer, a quaternary formation made up of alluvial deposits (Polytechnic College of Litoral (ESPOL) et al., 2014). The geological history of PRW begins at the Oligocene, where sedimentation of fine materials

originated the Tosagua formation. It comprises two members: Dos Bocas and Villingota. First, brown shales of Dos Bocas member were deposited. Later, the tuff shales were deposited to form Villingota member. Then in the upper Miocene, sandstones and silty clays of the Onzole formation were deposited. After, in the upper Miocene and Pliocene, sediments of Borbon formation were deposited. Finally, during the quaternary, a period of submersion happened favoring the formation of terraces followed by the deposition of alluvial material that continues in modern times. From the Portoviejo and Chico rivers confluence, a fluvial plain is shaped that reaches the Pacific Ocean. The fluvial plain has a variable width between 1km and 5km and a length of 20km, spreading south of Portoviejo city (Burbano et al., 2006).

There are two main relief areas that define the anthropic occupation: 1) fluvial plains, located from the center to the north, are characterized as smooth reliefs, with altitudes varying between 0 and 40 meters. 2) Elevations hills, located at the east of the watershed with maximum altitudes around 600 m. This region has low urbanization density, the main activity of this sector agriculture and livestock raising (Romano & Coral, 2020)

3. Materials and methods.

A methodology to calculate groundwater recharge for the next fifty years in the PRW was developed. This method uses water budgets adapted from (Fenn et al., 1975) (Figure 2). First, a runoff for the entire watershed was obtained. Second, two water balance conditions (for RCP 4.5 and RCP 8.5 emissions scenarios) for each year from 2021 to 2070 and actual data (from 1985 to 2005) were developed, and decadal groundwater recharge means were obtained. The entire work was divided into two stages, described below.

The first stage consists of a runoff map generated for the entire watershed using soil permeability, land cover use, and slope terrain shapefiles. Twelve classes of zones were obtained from previous information, with runoff coefficient ranges from 0.1 to 0.6, using the same criteria of Galvão et al. (2018). This geoprocessing was made in QGIS 3.4.0. An assumption in this work is that runoff will be constant over the next fifty years.

The second stage was the annual water balances calculation, using Thornthwaite and Mather method (C. Thornthwaite & Mather, 1955). A code in R using sf, dplyr, and tidyr libraries was created in this stage. Input data were future precipitation and temperature data (from ensembles of GCM), the latitude of PRW (to estimate the number of monthly sunlight duration), the runoff map from the first stage, and field capacity of PRW according to use and permeability of the soil. The result from this stage were one hundred shapefiles of groundwater recharge spatial distribution from

2021 to 2070 for PRW, also groundwater recharge for historical precipitation and temperature was calculated. Finally, shapefiles from previous stages were rasterized and averaged every 10 years. Changes in groundwater recharge (in mm) were calculated for each decade.

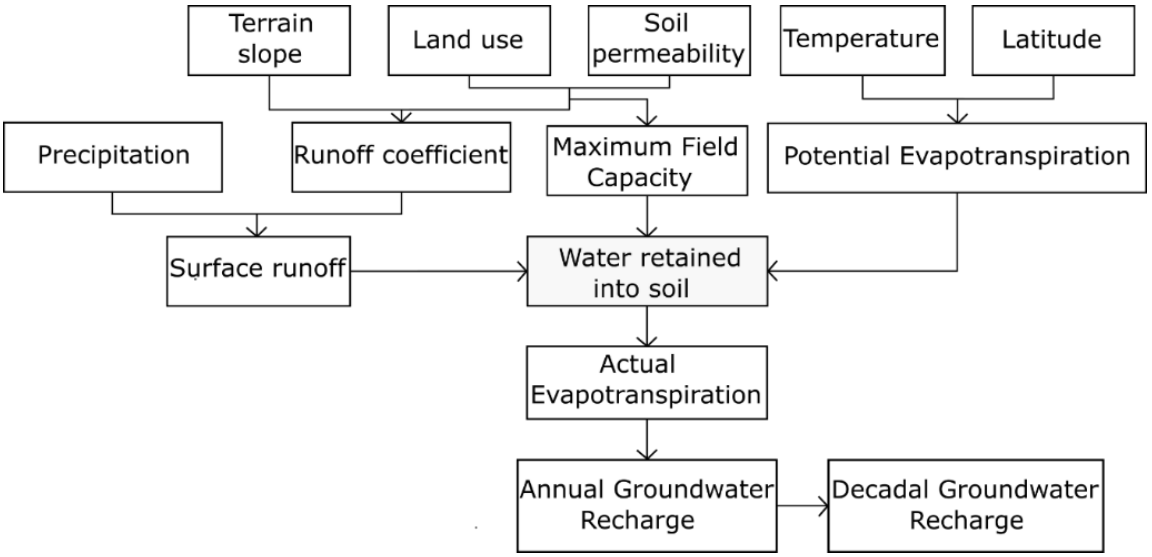


Figure 2.- Methodological scheme used in the present study.

3.1 Runoff map generation.

3.1.1.- Soil permeability map.

A pedological map with twelve types of soil, obtained from (The Geographic Military Institute, 2013) were reclassified into two classes according to its permeability characteristics. The criteria to classify soil was the size of particles according to (FAO, 1990). Soils with a high presence of coarse or medium-size particles were classified as high permeability soil (HPS); on the other hand, soils with fine particles were classified as low permeability soil (LPS). N/A means largely populated areas or water bodies. The soil reclassification is presented in figure 3.

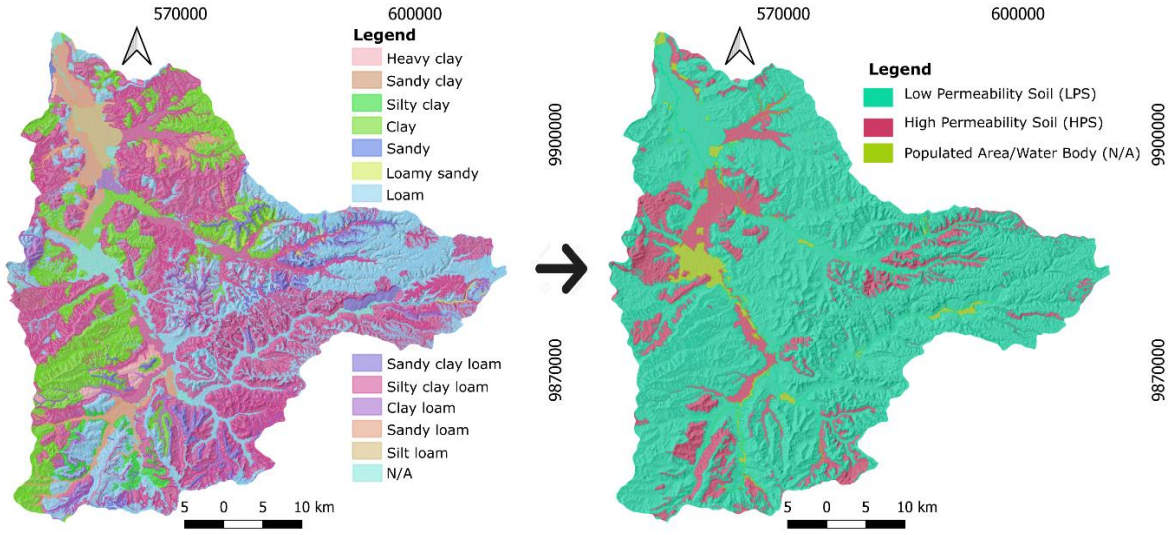


Figure 3.- Reclassification of pedological map of PRW (left) in two soil permeabilities (right).

3.1.2.- Land cover infiltration map.

The use of the soil map of PRW was studied and reclassified in two categories according to its capacity to retain water to infiltrate. Farmhouses, anthropic infrastructure, and soil use that reduce groundwater recharge were considered anthropic or areas with reduced groundwater recharge Owuor et al. (2016). On the other hand, the use of soil with high groundwater recharge was considered a forest or conserved area category. In addition, water bodies and unknowns were classified as a third category because it is impossible to calculate groundwater recharge using the proposed methodology for these soil uses. Land cover data and soil type data were obtained from (The Geographic Military Institute, 2013), which correspond to the 2019 year. The land cover reclassification is presented in figure 4.

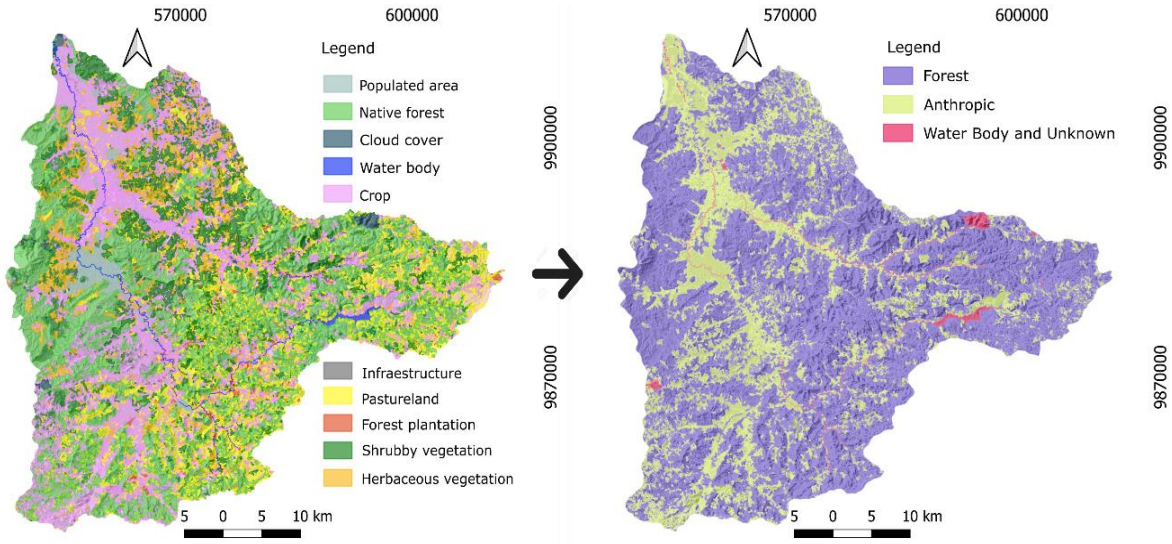


Figure 4.- Reclassification of land use map of PRW (left) in two kind of uses (right).

3.1.3.- Terrain slope map.

A Digital Elevation Model (DEM) provided by the STRM (Shuttle Radar Topography Mission), with a resolution of 1 arcsecond, was used to create a slope map reclassified in three intervals. Terrains with a slope lower than 2% were classified as flat; slopes higher than 2% and lower than 7% were classified as average; slopes higher than 7% were classified as steep, as was proposed in (Chow, 1965). The terrain slope is presented in figure 5.

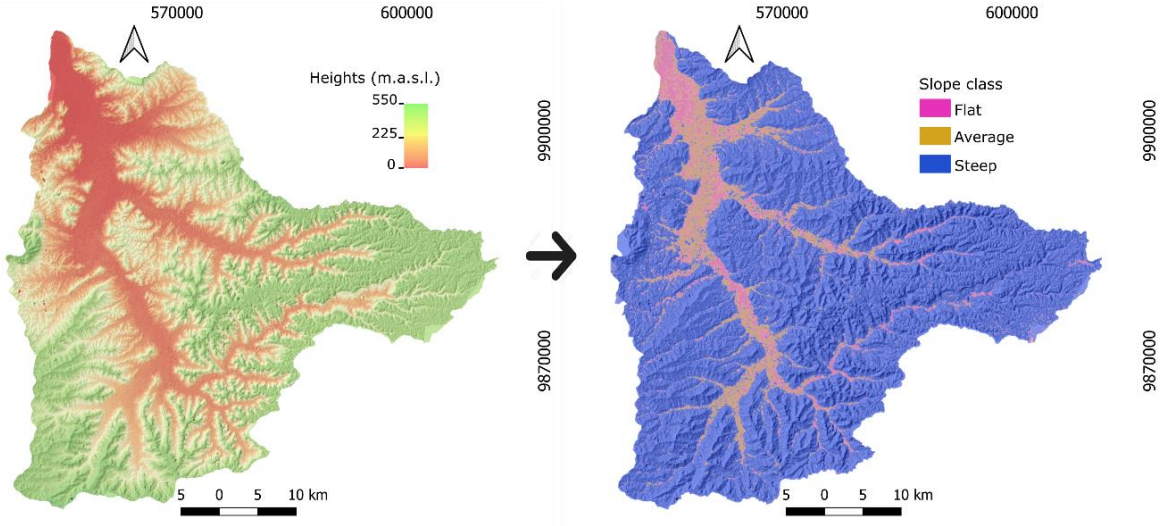


Figure 5.- Reclassification of PRW DEM (left) in three slopes intervals (right)..

3.1.4. Surface runoff.

The reclassified shapefiles corresponding to soil permeability, landcover infiltration capacity, and terrain slope were joined in QGIS 3.4.0. Finally, a map of 12 classes was generated, where the runoff coefficient ranged from 0,1 to 0,6 (Figure 6). The criteria to assign a runoff coefficient to each class were proposed by Galvão et al. (2018) and were described in Table 1. Groundwater recharge calculations were made only for current rural zones. The largest urban zones were no taken into account..

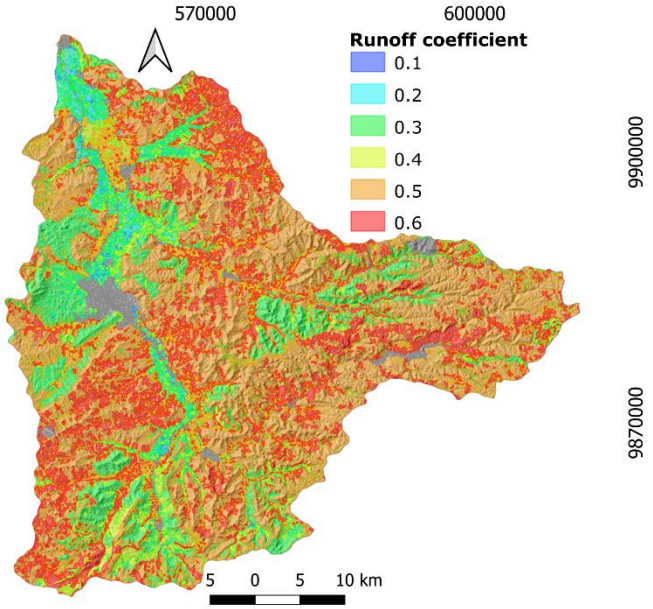


Figure 6.- Runoff spatial distribution in PRW.

Table 1.- Criteria to assign runoff coefficient to each class.

Class	Soil permeability	Land cover	Slope	Runoff coefficient
1	HPS	Forest/Conserved	Flat	0.1
2			Average	0.2
3			Steep	0.3
4		Anthropic	Flat	0.2
5			Average	0.3
6			Steep	0.4
7	LPS	Forest/Conserved	Flat	0.3
8			Average	0.4
9			Steep	0.5
10		Anthropic	Flat	0.4
11			Average	0.5
12			Steep	0.6

3.2.- Calculation of water balance.

The water balance method used in this study is one of the most used worldwide due to the simplicity of input variables (temperature, precipitation, field capacity of soil) and results coherence. The methodology allows calculating: runoff, percolation, actual evapotranspiration, soil water deficit, and excess. In this study, water balances for each year, according to runoff coefficient, and precipitation and temperature conditions in PRW were calculated. Water balance components according to the described methodology were: precipitation (P), surface runoff (SR), evapotranspiration (ET), and change in the storage soil (ΔS). The units of water balance components

were given in distance (mm). Described below each stage of water balance calculations, using Thornthwaite and Mather methodology, adapted to the study zone.

3.2.1.- Precipitation (P).

This component of the hydrological cycle represents the main inputs in the natural recharge of aquifers. Precipitation data were taken from future climatological scenarios from the Environment Ministry of Ecuador. These scenarios described in Armenta et al. (2016) were made from four GCM (IPSL-CM5A- MR, MIROC-ESM, GISS-E2-R, CSIRO-Mk3-6-0). Those models were subjected to a statistical downscaling using meteorological data collected in 137 stations between 1981 and 2005 from the INAMHI (Ecuador Meteorology and Hydrology National Institute). After downscaling, the final product was an ensemble of four climatological models. An ensemble combines climatological models that result in projections for a variable covering the future scenarios with the higher possibilities (Kotu & Deshpande, 2015). Mean precipitation in PRW, for the two RCP chosen is presented in figure 7 and figure 8.

A necessary input to develop climatological scenarios is an RCP, which assumes future emissions of greenhouse gasses. In the case of climatological data used for the present study, the RCP's chosen were 4.5 and 8.5. The first scenario assumes that emissions will reach their peak around the year 2040 and then decline, also assumes a stabilization of radiative forcing in 4.5 $\frac{W}{m^2}$ until 2100. The second scenario assumes increments of emissions each year. This scenario is called business as usual and causes a radiative forcing of 8.5 $\frac{W}{m^2}$ until 2100, with an increment in global temperature of 3°C (van Vuuren et al., 2011).

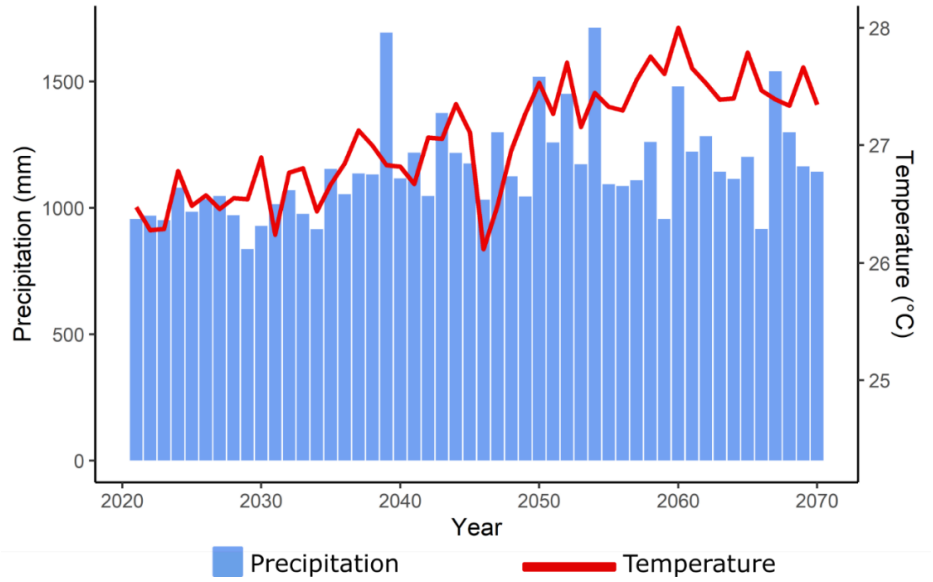


Figure 7.- Predicted annual mean of precipitation and temperature for PRW assuming a radiative forcing of 4.5 W/m^2

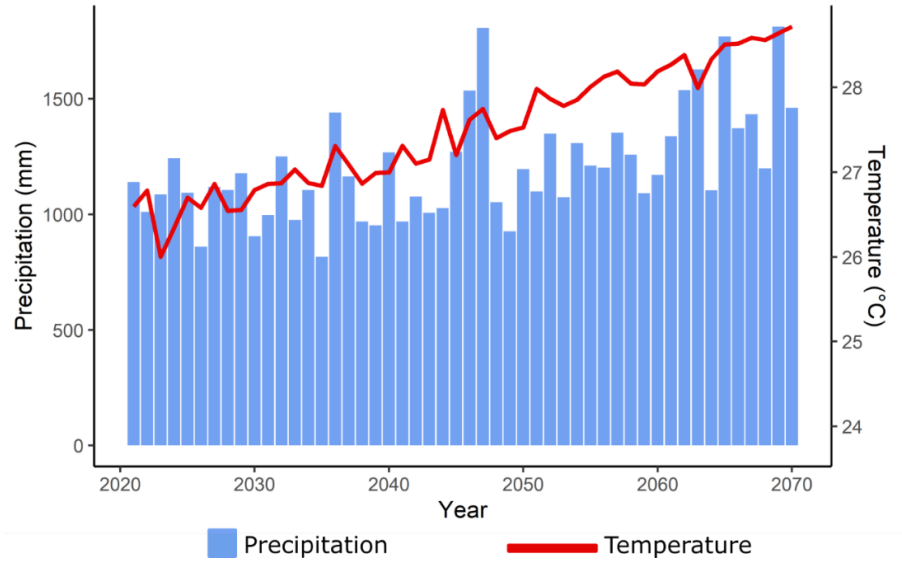


Figure 8.- Predicted annual mean of precipitation and temperature for PRW assuming a radiative forcing of 8.5 W/m^2

3.2.2.- Temperature (T).

This variable was obtained from future climate scenarios of the Environment Ministry of Ecuador, with the same methodology used for precipitation by (Armenta et al., 2016). The only difference respect to precipitation is the amount of INAMHI stations to make statistical downscaling; in the case of mean temperature32 stations were used, whereas in precipitation 137 were used.

3.2.3.- Potential evapotranspiration (PET).

It is the theoretical amount of water that could be converted into steam. Methodology to calculate PET was described in (Koerner & Daniel, 1997) as:

- A monthly index (Hm) was calculated, with 1.

$$H_m = (0.2T)^{1.514} \quad for\ T > 0 \quad (1)$$

Where:

T = Mean monthly temperature in Celsius degree.

- An annual index (Ha) for each year was calculated, which is sum of Hm:

$$H_a = \sum_{i=1}^{12} H_m \qquad (2)$$

- Unadjusted Potential Evapotranspiration (UPET) is obtained, with next equation.

$$UPET = 0.53 * (\frac{10T}{H_a})^a \ ;\ for\ T\ < 27 \qquad (3.1)$$

$$UPET = -0.015T^2 + 1{,}093T + 14.208 \ ;\ for\ T \geq 27 \qquad (3.2)$$

Where:

$$a = (6.75 * 10^{-7}) * H_a^3 - (6.75 * 10^{-5}) * H_a^2 + (0.01792) * H_a + 0.49239$$

Adjusted Potential Evapotranspiration (APET) was obtained multiplying UPET by the mean monthly sunlight duration (N), corrected and expressed in units of 12 hours periods; this value depends on latitude and month of the year, for the case of PRW values of N are described in Table 2:

Table 2.- Values of mean possible monthly duration of sunlight corrected and expressed in units of 12 hours periods (N) for PRW.

Month	N
January	31.2
February	28.2
March	31.2
April	30.3
May	31.2
June	30.2
July	31.2
August	31.2
September	30.3
October	31.2
November	30.3
December	31.2

3.2.4.- Surface runoff (SR).

It is the multiplication of the runoff coefficient (obtained in section 3.1) and precipitation (P, obtained in section 3.2.1), and represents the amount of water drainage to the nearest stream channel.

3.2.5.- Water retained into the soil (WRS)

It is the water into the soil after a precipitation event. In terms of the methodology, it is the difference between P and SR. WRS could be: taken by plants for transpiration, converted into evaporation, be part of sub-superficial runoff or percolate to the groundwater table.

3.2.6. Water retained into soil-less potential evaporation (WSPE).

This step is checked if there is a monthly excess or deficit of humidity in the soil. If the value is negative, the soil is drying. On the other hand, if the value is positive indicates an accumulation of water. In terms of methodology is the difference between WRS and PET.

3.2.7. Accumulated water loss (AWL).

It is the sum of negative values of WSPE beginning in January; when WSPE is positive, AWL is zero.

3.2.8.- Field capacity (FC).

It is the maximum water amount into the soil that plants can tap for transpiration per month. To calculate that value is necessary to know the depth of the root zone. However, it is possible to

estimate FC according to kind and use of soil, as is showed in Table 3, which was taken from (C. W. Thornthwaite & Mather, 1957).

Table 3.- Field capacity (mm) according to use and type of soil, adapted from (Thornthwaite and Mather, 1957).

	Sandy	**Sandy loam**	**Silty loam**	**Clay loam**	**Silty**
Shallow-rooted plants	50	75	125	100	75
Moderately deep-rooted plants	75	150	200	200	50
Deep-rooted plants	100	150	250	250	200
Fruit	150	250	300	250	300
Mature forest	250	300	400	400	350

For the area of study, the spatial distribution of field capacity (FC) in mm is showed in Figure 9:

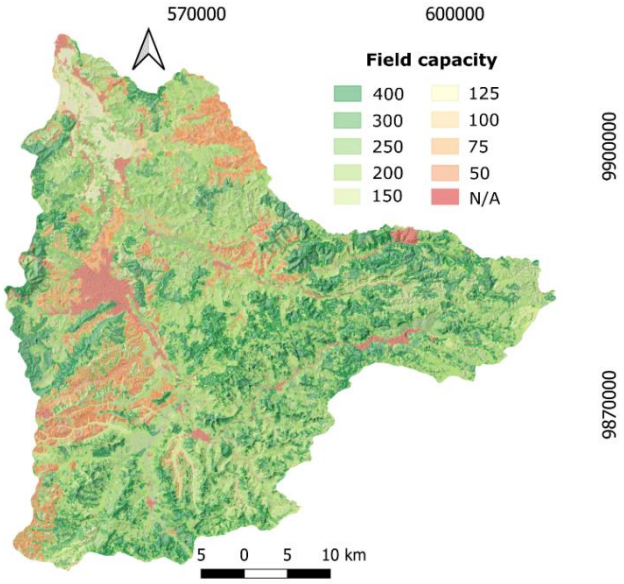


Figure 9.- Estimation of the spatial distribution of field capacity (FC) in PRW.

FC varies over time, according to climatological conditions, a monthly field capacity (MFC) is calculated for each month. To know MFC according to climatological conditions, the following equation is used.

$$MFC = (FC)10^{b(WSPE)} \qquad (4)$$

Where:

$$b = \frac{0.455}{FC}$$

3.2.9.- Field capacity changes (FCC).

It is defined as the difference of FC between months. When this value is positive, the amount of water in the soil increases. Whereas when it is negative, the soil is drying.

3.2.10.- Water deficit (WD).

This is obtained with the difference between WSPE and FCC when WSPE is negative. On the other hand, when WSPE is positive WD is zero.

3.2.11.- Actual evapotranspiration (AET).

It is obtained subtracting PET and WD when WSPE is negative. On the other hand, when WSPE is positive, AET is the same as PET. AET is the actual amount of water that is removed from the soil as vapor.

3.2.12.- Percolation.

Once the root zone is saturated, infiltration is higher than potential evapotranspiration. Then percolation to deeper zones becomes significant. It is represented by the difference between WSPE and WD when WSPE is positive.

3.3.- Groundwater recharge for next five decades.

Finally, a function in the programming language R was run. Input data were precipitation and temperature data from 2021 to 2070. Runoff and field capacity were assumed constant for the next fifty years. The function returned a shapefile with thirteen columns for each year, one per month and one with the annual groundwater recharge.

Annual shapefiles were rasterized. Next, a mean of ten years was obtained, plotted, and analyzed. In this stage, geographical operations were made in QGIS 3.4 software.

4.- Results and discussions.

4.1.- Runoff map results.

The spatial distribution of the runoff coefficient is shown in figure 6. Next, the results for each input variable are described.

4.1.1.- Soil permeability.

Results reflect that clay soils predominate in PRW. However, their presence is more noticeable in the upper zones of the basin. Around Portoviejo city, soils with medium-sized particles, such as clay loam and loam, are present; these are the most permeable soils in the area. This fact must be considered for the Integral Management of Water Resources in Development and Territorial Ordering Plans. In the upper zones of the Rocafuerte urban area, it is also possible to find Loamy Clay soils. Soils with coarse particles are scarce in the area; one of the most representative examples is the sandy loam soil found in the middle part of the basin, between the populated centers of Santa Ana and Portoviejo. Described results are presented in figure 3.

4.1.2.- Infiltration capacity by use of soil.

Land use is one of the leading human factors influencing groundwater systems (Fenn et al., 1975). In the basin, there is a land occupation conditioned by the topography. In figure 4, an anthropic occupation is noted in areas with low and medium slopes. Although the aquifer's recharge can be favored in flat areas, this effect can be canceled by the anthropic occupation in PRW. On the other hand, a clear relationship between the type and use of soil cannot be observed; in the areas classified as sandy soils (medium and coarse particles), different soil uses can be observed, from short-cycle crops to native and shrubby vegetation. Figure 4 describes results for the use of soil classification.

4.1.3.- Slope terrain.

Topography in the Portoviejo river basin reveals two valleys: the Chico river valley and the Portoviejo River valley. Both meet in the lower middle zone of the basin to a few kilometers from the urban of Portoviejo canton; land use in both valleys is cropping in both cases. It is noted that the areas with native vegetation are found in lands with high slopes, which could indicate that preservation in those areas is due to their difficult access and challenging conditions to develop agriculture. Described results are presented in figure 5.

4.1.4.- Integration of input variables.

Integration of the three previous maps derived in a map of 12 classes, whose runoff coefficient ranged from 0.1 to 0.6; the higher coefficient, the less precipitation is retained in the soil. Therefore, the possibilities of infiltration decrease.

In PRW, zones with a lower coefficient (0.1 to 0.2) are found in lower zones due to flat slopes and medium-size particle soils found in the sector. Zones with a coefficient of 0.3 surround the city of Portoviejo; this runoff coefficient was obtained due to medium-size particle soils and medium slopes found in the sector. However, land uses as crops do not favor the retention of rainfall in the soil. The spatial distribution of the runoff coefficient is shown in Figure 6.

Due to the presence of coarse and medium-sized particles in soils and medium slopes of the sector, runoff coefficients between 0.3 and 0.4 are found between Santa Ana and Olmedo. The same conditions are observed in higher rural zones of Portoviejo. Finally, high runoff coefficients (0.5 and 0.6) are distributed in most of the areas in PRW, especially in higher rural zones of Portoviejo canton and medium-low zones (Figure 6).

4.2.- Annual water balances.

Water balances from 2021 to 2070 for both scenarios are presented in figure 10 and figure 11. For both scenarios (RCP 4.5 and RCP 8.5), it is evident that groundwater recharge has the lowest amount of water among the hydrological cycles components for PWR. Groundwater recharge also is the water cycle component with highest interannual variability. For scenario RCP 4.5, there are four years with groundwater recharge rates higher than 100mm (2039, 2052, 2054 and, 2060), while for scenario RCP 8.5, there are ten years with values higher than 100 mm (2036, 2046, 2047, 2057, 2062, 2063, 2065, 2067, 2069, 2070).

It is necessary to highlight that due to the assumption that runoff and FC will be constant for the next fifty years, recharge values (figure 10 and figure 11) could change drastically. However, figure 10 and figure 11 point out that predicted relative changes in groundwater recharge would be greater than the corresponding changes in mean precipitation, suggesting an amplification of climate change impacts in groundwater systems (Ng et al., 2010).

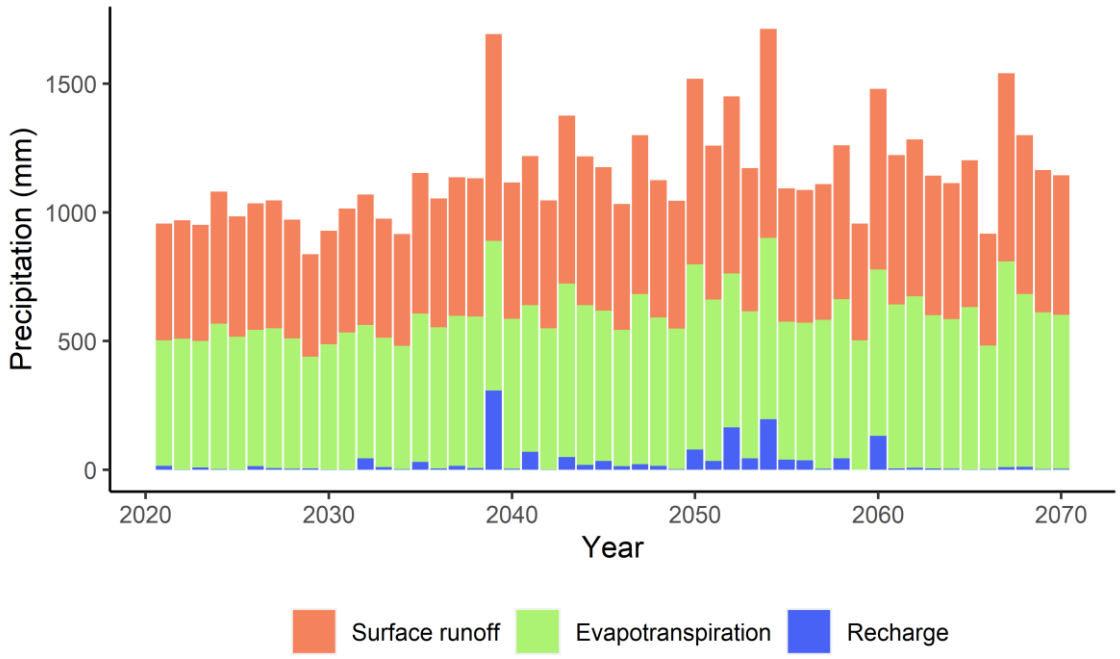


Figure 10.- Water Budgets for years from 2021 to 2070 in PRW (RCP 4.5)

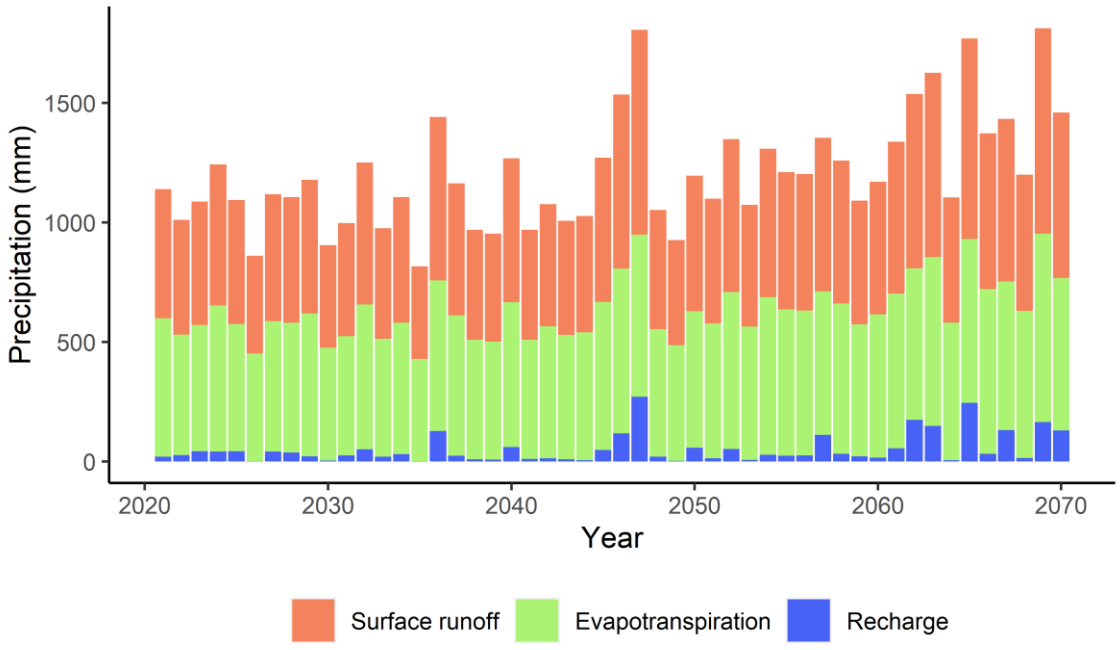


Figure 11.- Water Budgets for years from 2021 to 2070 in PRW (RCP 8.5)

4.3.- Current groundwater recharge.

Input data for the current scenario were historical data of precipitation and temperature. Higher groundwater recharge zones (>= 75 mm/year) are located in rural zones of Portoviejo. Currently, this location does not have access to a public water provision; wells are the primary water source

in the sector. Therefore, a reduction in recharge rates could be mean a crisis in the water provision for the rural communities. Recharge rate between 50 mm/year and 75 mm/year is found to the north of the current Portoviejo city, and this is the highest rate in the lower zone of the watershed. Taking account this information is necessary for the correct management of this area. The recharge rate near the mouth of the watershed is between 25 mm/year and 50 mm/year; if the extraction is higher than recharge could marine intrusion could happen.

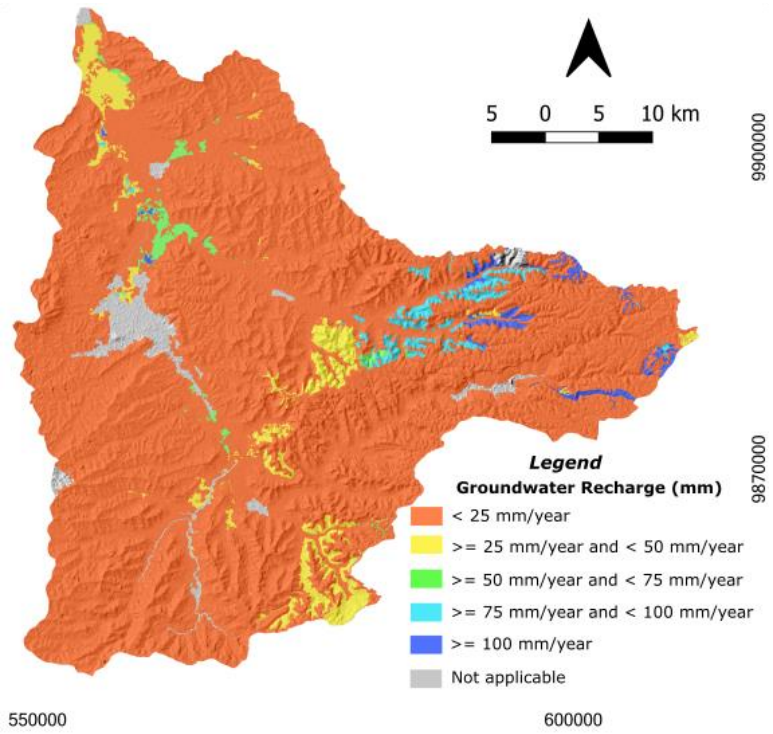


Figure 12.- Mean recharge from 1985 to 2005.

4.4.- Decadal means for future groundwater recharge.

Figure 13 shows the results under scenario RCP 4.5. It is possible to appreciate that groundwater recharge zones in PRW are not spatially constant. For the decade 2021 – 2030, in the higher rural zones of Portoviejo and Santa Ana, there is a decline in groundwater recharge rates that may lead to groundwater reserve depletion. It is necessary to highlight that this zone does not have a public water supply service and private wells are the primary water source during the dry season. Droughts are expected for the next decade in the sector that may increase water consumption further depleting groundwater reserves. Groundwater recharge zones located to the north of Portoviejo city are maintained. However, it is necessary to consider that expansion of the town could provoke a reduction of permeability in the sector. Finally, groundwater recharge near the watershed mouth will decrease until 25 mm/year for the decade analyzed. An increment in groundwater intrusion is expected in the sector.

For 2031- 2040, groundwater recharge will increase in the entire watershed, and potential future groundwater recharge zones are found. These zones are generally found in the valley between Portoviejo and Santa Ana, around Portoviejo city, and the high zones of Portoviejo and Santa Ana. For valley between Portoviejo and Santa and Portoviejo city, it´s recommended to carry out a planned urban expansion; several regions are transitioning from rural to urban zones. In the case of the high rural zones of Portoviejo, soil impermeabilization must be avoided. For zones near the watershed mouth, the recharge will increase compared to 2021 – 2030 and the current scenario; this could be taken as an advantage to face future advances of the saltwater wedge due to the sea level rise. Finally, for the rest of the watershed, groundwater recharge will increase until 50 mm/year.

For 2041-2050, zones with a higher groundwater recharge rate are the same as the previous decade. However, areas with a recharge between 25 mm/year and 50 mm/year are reduced. This fact reaffirms the need to correctly manage the use of soil in the identified zones previously. For 2051-2061, the spatial distribution of groundwater recharge rate is similar to 2031-2041. However, there is an increment of areas covering a groundwater recharge rate higher than 100 mm/year around Portoviejo.

From 2061-2070, the mean of groundwater recharge will decrease compared with the three previous decades. This fact is because higher zones inside the watershed have had lower value respect all the last decades, which could mean a severe water crisis in that zones. However, in lower zones of the watershed, higher groundwater recharge rates are maintained.

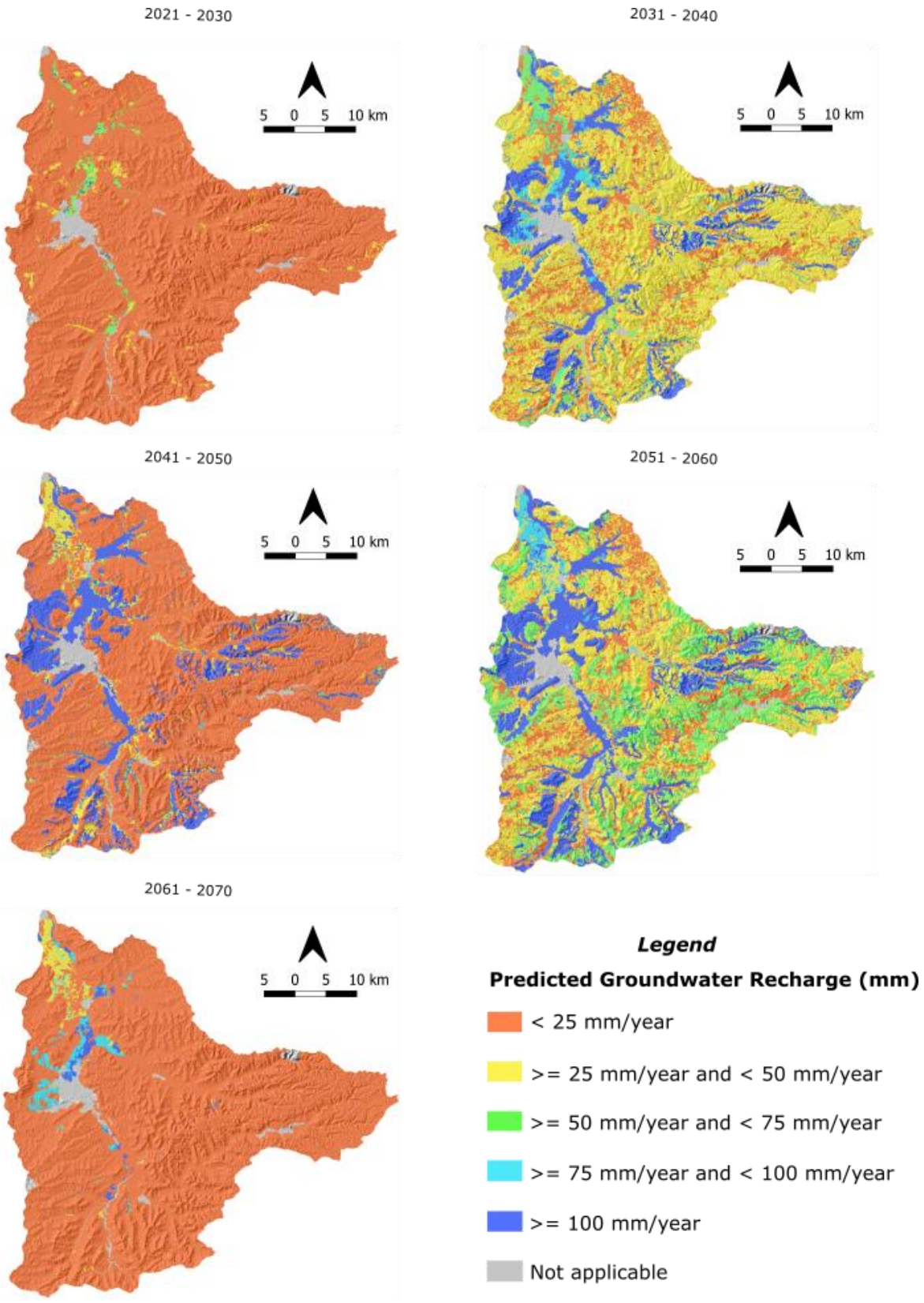


Figure 13.- Decadal groundwater recharge rates under the scenario RCP 4.5.

In figure 14 shows the results under scenario 8.5. For the decade 2021-2030 is possible to appreciate that scenario 8.5 offers better conditions for groundwater recharge. Zones where the

water reaches the aquifer, are the same as the most humid decades from scenario 4.5. Additional to the mentioned areas, scenario RCP 8.5 also favor recharge in high zones of the Portoviejo with rates until 75 mm/year. For the next three decades (2031 – 2060), patterns in the spatial distribution of groundwater recharge are similar to the decade 2021- 2030. However, there are slight differences in magnitude between the three decades. For the decade 2061-2070, groundwater is higher than the others, which could provoke floods without the correct use of soil.

Comparing scenarios RCP 4.5 and RCP 8.5, it is possible to realize that there are similitudes in the spatial distribution of higher groundwater recharge zones. For decades 2021-2031, 2041- 2050, and 2061-2070, scenario 8.5 favors the groundwater recharge of more millimeters, while scenario 4.5 favors an enhance groundwater recharge for decades 2031-2040 and 2051-2060. Although there is higher precipitation under RCP 8.5, this scenario does not always favor the most recharge; under scenario 8.5, a higher mean temperature increases evapotranspiration. Also, under scenario 8.5, there is a higher interannual variability of groundwater recharge.

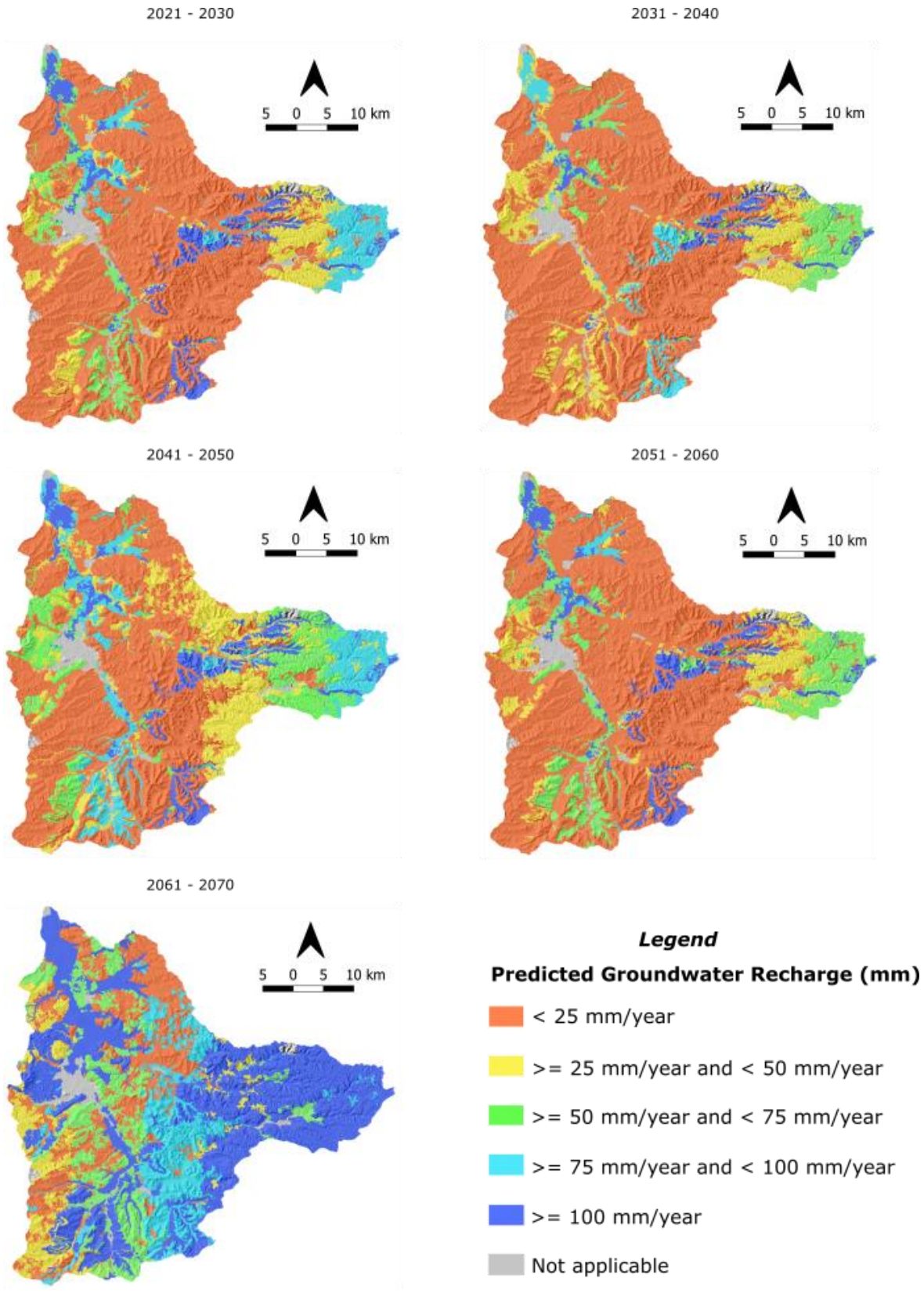


Figure 14.- Decadal groundwater recharge rates under the scenario RCP 8.5.

5. Conclusions

This study has established future groundwater recharge under the context of climate change, using annual water balances with Thornthwaite methodology for RCP 4.5 and RCP 8.5 models. QGIS and programming language R were software used for the development of the described method. According to the RCP 4.5 scenario, groundwater recharge zones in PRW will change spatially because of changes in precipitation and temperature regime; between 2031 and 2060, groundwater recharge will increase in almost the entire watershed. On the other hand, in the higher rural zones of Portoviejo, groundwater recharge will decrease in decades 2021-2030 and 2061-2070. For RCP 8.5, results show that groundwater recharge zones will be the same until 2060. In general terms, higher groundwater recharge zones are the same for both scenarios. However, a higher interannual variability is seen for scenario RCP 8.5. Results from the present study could provide information for the creation of Territorial Ordering Plans. Therefore, it is necessary to identify field parameters of the aquifer (permeability, conductivity, storage coefficient) to know how the spatial changes in groundwater recharge patterns will affect the availability and quality of groundwater resources.

References

Armenta, G., Villa, J., & Jácome, P. (2016). *Proyecciones Climáticas de Precipitación y Temperatura para Ecuador, Bajo Distintos Escenarios de Cambio Climático.*

Boufekane, A., Meddi, H., & Meddi, M. (2020). Delineation of groundwater recharge zones in the Mitidja plain, north Algeria, using multi-criteria analysis. *Journal of Hydroinformatics*, *22*(6), 1468–1484. https://doi.org/10.2166/HYDRO.2020.082

Burbano, N., Becerra, S., & Pasquel, E. (2006). *Caracterización Hidrogeológicas de las cuencas Portoviejo - Chone*. https://issuu.com/inamhi/docs/caract._hidrogeologica-manabi/29

Carrión, P., Herrera, G., Briones, J., Sánchez, C., & Limón, J. (2018). Practical adaptations of ancestral knowledge for groundwater artificial recharge management of Manglaralto coastal aquifer, Ecuador. *WIT Transactions on Ecology and the Environment*, *217*, 375–386. https://doi.org/10.2495/SDP180341

Chen, Z., Grasby, S. E., & Osadetz, K. G. (2002). Predicting average annual groundwater levels from climatic variables: An empirical model. *Journal of Hydrology*, *260*(1–4), 102–117. https://doi.org/10.1016/S0022-1694(01)00606-0

Chow, V. Te. (1965). Handbook of applied hydrology. *International Association of Scientific Hydrology. Bulletin*, *10*(1), 82–83. https://doi.org/10.1080/02626666509493376

Chowdhury, A., Jha, M. K., & Chowdary, V. M. (2010). Delineation of groundwater recharge zones and identification of artificial recharge sites in West Medinipur district, West Bengal, using RS, GIS and MCDM techniques. *Environmental Earth Sciences*, *59*(6), 1209–1222. https://doi.org/10.1007/s12665-009-0110-9

Conicelli, B., Hirata, R., Galvão, P., Bernardino, M., Simonato, M., Abreu, M. C., Aranda, N., & Terada, R. (2021). Determining groundwater availability and aquifer recharge using GIS in a highly urbanized watershed. *Journal of South American Earth Sciences*, *106*(September 2020). https://doi.org/10.1016/j.jsames.2020.103093

CRM, INERHI, & CONADE. (1991). *Plan Integral de Desarrollo de los Recursos Hídricos de la Provincia de Manabí*. https://www.oas.org/dsd/publications/Unit/oea40s/oea40s.pdf

Ehtiat, M., Jamshid Mousavi, S., & Srinivasan, R. (2018). Groundwater Modeling Under Variable Operating Conditions Using SWAT, MODFLOW and MT3DMS: a Catchment Scale Approach to Water Resources Management. *Water Resources Management*, *32*(5), 1631–1649.

https://doi.org/10.1007/s11269-017-1895-z

FAO. (1990). Guidelines for profile description. In *Guidelines for profile description*. http://www.fao.org/tempref/FI/CDrom/FAO_Training/FAO_Training/General/x6706s/x6706s06.htm#top

Fenn, D., Hanley, K., & DeGeare, T. (1975). *Use of the water-balance method for predicting leachate generation from solid-waste-disposal sites* (p. 40). http://www.osti.gov/scitech/biblio/6328350

Fisher, J. C., Bartolino, J. R., Wylie, A. H., Sukow, J., & McVay, M. (2016). Groundwater-Flow Model for the Wood River Valley Aquifer System, South-Central Idaho. In *Scientific Investigations Report*. http://pubs.er.usgs.gov/publication/sir20165080

Galvão, P., Hirata, R., & Conicelli, B. (2018). Estimating groundwater recharge using GIS-based distributed water balance model in an environmental protection area in the city of Sete Lagoas (MG), Brazil. *Environmental Earth Sciences*, *77*(10), 1–19. https://doi.org/10.1007/s12665-018-7579-z

Giler-Ormaza, A. (2018). A province with several climates: What knowledge of hydrology can be useful? A literature review. *Maskana*, *9*(2), 41–51. https://doi.org/10.18537/mskn.09.02.06

Guevara-Ochoa, C., Medina-Sierra, A., & Vives, L. (2020). Spatio-temporal effect of climate change on water balance and interactions between groundwater and surface water in plains. *Science of the Total Environment*, *722*. https://doi.org/10.1016/j.scitotenv.2020.137886

Hirata, R., & Conicelli, B. P. (2012). Groundwater resources in Brazil: A review of possible impacts caused by climate change. *Anais Da Academia Brasileira de Ciencias*, *84*(2), 297–312. https://doi.org/10.1590/S0001-37652012005000037

Holger, T., Martin-Bordes, J. L., & Gurdak, J. J. (2012). *Climate Change Effects on Groundwater Resources A Global Synthesis of Findings and Recommendations* (T. Holger, J. L. Martin-Bordes, & J. J. Gurdak (eds.)). CRC Press/Balkema. https://groundwaterportal.net/sites/default/files/Climate change effects on groundwater resources - A global synthesis of findings and recommendations.pdf

Holman, I. P. (2006). Climate change impacts on groundwater recharge-uncertainty, shortcomings, and the way forward? *Hydrogeology Journal*, *14*(5), 637–647. https://doi.org/10.1007/s10040-005-0467-0

Jackson, C. (2012). *Future Flows and Groundwater Levels: R-Groundwater model summary*. http://nora.nerc.ac.uk/id/eprint/20778/1/CR12105N.pdf

Koerner, R., & Daniel, D. (1997). Final Covers for Solid Waste Landfills and Abandoned Dumps. In *Final Covers for Solid Waste Landfills and Abandoned Dumps*. https://doi.org/10.1680/fcfswlaad.9780784402610

Kotu, V., & Deshpande, B. (2015). Data Mining Process. In V. Kotu & B. Deshpande (Eds.), *Predictive analytics and data mining: Concepts and practice with RapidMiner* (1st ed., pp. 17–36). Morgan Kaufmann. https://www.sciencedirect.com/science/article/pii/B9780128014608000021

Magesh, N. S., Chandrasekar, N., & Soundranayagam, J. P. (2012). Delineation of groundwater potential zones in Theni district, Tamil Nadu, using remote sensing, GIS and MIF techniques. *Geoscience Frontiers*, *3*(2), 189–196. https://doi.org/10.1016/j.gsf.2011.10.007

National Institute of Statistics and Censuses (INEC). (2010). *Population and Housing National Census*.

Ng, G.-H. C., McLaughlin, D., Entekhabi, D., & Scanlon, B. R. (2010). Probabilistic analysis of the effects of climate change on groundwater recharge. *Water Resources Research*, *46*(7), 1–18. https://doi.org/10.1029/2009wr007904

Owuor, S. O., Butterbach-Bahl, K., Guzha, A. C., Rufino, M. C., Pelster, D. E., Díaz-Pinés, E., & Breuer, L. (2016). Groundwater recharge rates and surface runoff response to land use and land cover changes in semi-arid environments. *Ecological Processes*, *5*(1). https://doi.org/10.1186/s13717-016-0060-6

Polytechnic College of Litoral (ESPOL), Ecuador Water National Secretary, & Spanish Agency for the International Development Cooperation. (2014). *ELABORACIÓN DEL MAPA HIDROGEOLÓGICO A ESCALA 1 : 250.000*. shorturl.at/gsyKL

Romano, J., & Coral, B. V. (2020). Public management, private management and collective action in the Portoviejo River Basin: Visions and conflicts. *Sustainability (Switzerland)*, *12*(13). https://doi.org/10.3390/su12135467

Rukundo, E., & Doğan, A. (2019). Dominant influencing factors of groundwater recharge spatial patterns in Ergene river catchment, Turkey. *Water (Switzerland)*, *11*(4). https://doi.org/10.3390/w11040653

Saiz-Rodríguez, J. A., Lomeli Banda, M. A., Salazar-Briones, C., Ruiz-Gibert, J. M., & Mungaray-Moctezuma, A. (2019). Allocation of groundwater recharge zones in a rural and semi-arid region for sustainable water management: Case study in Guadalupe Valley, Mexico. *Water (Switzerland)*, *11*(8). https://doi.org/10.3390/w11081586

Scanlon, B. R., Healy, R. W., & Cook, P. G. (2002). Choosing appropriate techniques for quantifying groundwater recharge. *Hydrogeology Journal*, *10*(1), 18–39. https://doi.org/10.1007/s10040-001-0176-2

Senanayake, I. P., Dissanayake, D. M. D. O. K., Mayadunna, B. B., & Weerasekera, W. L. (2016). An approach to delineate groundwater recharge potential sites in Ambalantota, Sri Lanka using GIS techniques. *Geoscience Frontiers*, *7*(1), 115–124. https://doi.org/10.1016/j.gsf.2015.03.002

Singh, A., Panda, S. N., Kumar, K. S., & Sharma, C. S. (2013). Artificial groundwater recharge zones mapping using remote sensing and gis: A case study in Indian Punjab. *Environmental Management*, *52*(1), 61–71. https://doi.org/10.1007/s00267-013-0101-1

Taheri, A., & Voudouris, K. S. (2007). Groundwater quality in the semi-arid region of the Chahardouly basin, West Iran. *HYDROLOGICAL PROCESSES*, *22*(October 2007), 3066–3078. https://doi.org/10.1002/hyp

Thampi, S. G., & Raneesh, K. Y. (2011). Impact of anticipated climate change on direct groundwater recharge in a humid tropical basin based on a simple conceptual model. *Hydrological Processes*, *26*, 1655–1671. https://onlinelibrary.wiley.com/doi/epdf/10.1002/hyp.8285

Thapa, R., Gupta, S., Guin, S., & Kaur, H. (2017). Assessment of groundwater potential zones using multi-influencing factor (MIF) and GIS: a case study from Birbhum district, West Bengal. *Applied Water Science*, *7*(7), 4117–4131. https://doi.org/10.1007/s13201-017-0571-z

The Geographic Military Institute. (2013). *Agricultural Public Information System*. http://geoportal.agricultura.gob.ec/index.php/geoservicios1

Thielen, D., Cevallos, J., Erazo, T., Zurita, I. S., Figueroa, J., Matute, N., Quintero, J. I., Agropecuarias, D. C., & Ambiente, D. M. (2016). Dinámica espacio-temporal de las precipitaciones durante el evento de El Niño 97 / 98 en la cuenca de Río Portoviejo , Manabí , costa ecuatoriana del Pacífico. *Revista de Climatología*, *16*(February), 35–50.

Thornthwaite, C., & Mather, J. (1955). The water balance. In *Stanford Library* (VIII, Issue 236).

https://doi.org/10.1201/9780203751435-9

Thornthwaite, C. W., & Mather, J. R. (1957). Instructions and Tables for Computing Potential Evapotranspiration and Water Balance. *Publications in Climatology*, *10*, 185–311.

Tilahun, K., & Merkel, B. J. (2009). Estimation of groundwater recharge using a GIS-based distributed water balance model in Dire Dawa, Ethiopia. *Hydrogeology Journal*, *17*(6), 1443–1457. https://doi.org/10.1007/s10040-009-0455-x

van Vuuren, D. P., Edmonds, J., Kainuma, M., Riahi, K., Thomson, A., Hibbard, K., Hurtt, G. C., Kram, T., Krey, V., Lamarque, J. F., Masui, T., Meinshausen, M., Nakicenovic, N., Smith, S. J., & Rose, S. K. (2011). The representative concentration pathways: An overview. *Climatic Change*, *109*(1), 5–31. https://doi.org/10.1007/s10584-011-0148-z

Yeh, H. F., Cheng, Y. S., Lin, H. I., & Lee, C. H. (2016). Mapping groundwater recharge potential zone using a GIS approach in Hualian River, Taiwan. *Sustainable Environment Research*, *26*(1), 33–43. https://doi.org/10.1016/j.serj.2015.09.005

Zomlot, Z., Verbeiren, B., Huysmans, M., & Batelaan, O. (2017). Trajectory analysis of land use and land cover maps to improve spatial–temporal patterns, and impact assessment on groundwater recharge. *Journal of Hydrology*, *554*, 558–569. https://doi.org/10.1016/j.jhydrol.2017.09.032

Appendices.

Appendix A.

Code for transforming .nc files to indicidual rasters (.tif) in R.

```
setwd("C:/Portoviejo/base/Hist/rstr") ##set working directory

library(raster) ##active raster library in R

for (i in 2021:2070){ #create a loop from 2021 to 2070

  ncpath <- "C:/Portoviejo/base/Hist/" ##insert path where tif´s are found

  ncnamep <- "pr_day_Ecuador_Ensamble_" # insert pattern of precipitation files (.nc)

  ncnamet <- "tas_day_Ecuador_Ensamble_"   # insert pattern of temperature files (.nc)

  ncfnamep <- paste(ncpath,ncnamep,i,".nc", sep="")

  ncfnamet <- paste(ncpath,ncnamet,i,".nc", sep="")

  prec_raster <- brick(ncfnamep, varname="precip") ##read precipitation files (.nc)

  temp_raster <- brick(ncfnamet, varname="temp") ##read temperature files (.nc)

  month <- c("January","February","March","April","May","June",
"July","August","September","October","November","December")

  l  <- c(31,29,31,30,31,30,31,31,30,31,30,31)

  t1 <- temp_raster/l

  p1 <- prec_raster

for(j in 1:length(month)){ ##create a name for each monthly .tif

    m <- month[j]

    namep <- paste(m,"_prec_",i,".tif",sep = "")

    namet <- paste(m,"_temp_",i,".tif",sep = "")

    r <- subset(t1,j)

    r2 <- subset(p1,j)

    writeRaster(r, filename = namet)  ##save monthy temperature raster
```

```
   writeRaster(r2, filename = namep) ##save monthly precipitation raster
  }
}
```

Appendix B.

Code for transforming rasters (.tif) to shapefiles in R.

```
library(sf)
library(raster)
library(dplyr)
for(i in 21:70){
  setwd("C:/Portoviejo/Cambio_climatico/RCP85/rstr2")
  n <- paste("prec_20",i,".tif", sep = "")
  nt <- paste("temp_20",i,".tif", sep = "")
  ntf <- paste("temp_20",i,".gpkg", sep = "")
  nf <- paste("prec_20",i,".gpkg", sep = "")
  files_prec  <- list.files(pattern = n) ##create a list with patterns of precipitation rasters
  files_temp  <- list.files(pattern = nt) ##create a list with patterns of temperature rasters
  prec <- lapply(files_prec,raster) ##apply raster function to each  precipitation file in the list
  temp <- lapply(files_temp,raster) ##apply raster function to each temperature file in the list
  ec_prec <- lapply(prec,rasterToPolygons, n = 4)##transform precipitation rasters to shapefiles
  ec_temp <- lapply(temp, rasterToPolygons, n = 4) ## transform temperature rasters to shapefiles
  dp <- st_as_sf(ec_prec[[1]]) ##extract the first monthly precipitation shapefiles
  dt <- st_as_sf(ec_temp[[1]]) ##extract the first monthly temperature shapefiles
  p <- lapply(ec_prec, as.data.frame) ##transform to dataframe monthly precipitation files
  t <- lapply(ec_temp, as.data.frame) ##transform to dataframe monthly temperature files
```

```
 ft <- inner_join(dp,p) #join spatial data with dataframes to create a annual precipitaion shapefiles

 fp <- inner_join(dt,t) #join spatial data with dataframes to create a annual temperature shapefiles

 setwd("C:/Portoviejo/Cambio_climatico/RCP85/gpkgc") # change woking directory to save shapefiels

 write_sf(ft,ntf)

 write_sf(fp,nf)

}
```

Appendix C.

Code for creating a function to obtain possible monthly duration of sunlight corrected and expressed in units of 12 hours periods.

```
latitude <- function(lat ,hem){

a1 <- c(0, 31.2, 28.2, 31.2, 30.3, 31.2, 30.3, 31.2, 31.2, 30.3, 31.2, 30.3, 31.2)

a2 <- c(1, 31.2, 28.2, 31.2, 30.3, 31.2, 30.3, 31.2, 31.2, 30.3, 31.2, 30.3, 31.2)

a3 <- c(2, 31.5, 28.2, 31.2, 30.3, 30.9, 30.0, 31.2, 31.2, 30.3, 31.2, 30.6, 31.5)

a4 <- c(3, 31.5, 28.5, 31.2, 30.0, 30.9, 30.0, 30.9, 31.2, 30.0, 31.2, 30.6, 31.5)

a5 <- c(4, 31.8, 28.5, 31.2, 30.0, 30.9, 29.7, 30.9, 30.9, 30.0, 31.5, 30.6, 31.8)

a6 <- c(5, 31.8, 28.5, 31.2, 30.0, 30.6, 29.7, 30.6, 30.9, 30.0, 31.5, 30.9, 31.8)

a7 <- c(6, 31.8, 28.8, 31.2, 30.0, 30.6, 29.4, 30.6, 30.9, 30.0, 31.5, 30.9, 32.1)

a8 <- c(7, 32.1, 28.8, 31.2, 30.0, 30.6, 29.4, 30.3, 30.6, 30.0, 31.5, 30.9, 32.4)

a9 <- c(8, 32.1, 28.8, 31.5, 29.7, 30.3, 29.1, 30.3, 30.6, 30.0, 31.8, 31.2, 32.4)

a10 <- c(9, 32.4, 29.1, 31.5, 29.7, 30.3, 29.1, 30.0, 30.6, 30.0, 31.8, 31.2, 32.7)

a11 <- c(10, 32.4, 29.1, 31.5, 29.7, 30.3, 28.8, 30.0, 30.3, 30.0, 31.8, 31.5, 33.0)

a12 <- c(11, 32.7, 29.1, 31.5, 29.7, 30.0, 28.8, 29.7, 30.3, 30.0, 31.8, 31.5, 33.0)

a13 <- c(12, 32.7, 29.1, 31.5, 29.7, 30.0, 28.5, 29.7, 30.3, 30.0, 31.8, 31.8, 33.3)
```

```
a14 <- c(13, 33.0, 29.4, 31.5, 29.4, 29.7, 28.5, 29.4, 30.0, 30.0, 32.1, 31.8, 33.3)

a15 <- c(14, 33.3, 29.4, 31.5, 29.4, 29.7, 28.2, 29.4, 30.0, 30.0, 32.1, 32.1, 33.6)

a16 <- c(15, 33.6, 29.4, 31.5, 29.4, 29.4, 28.2, 29.1, 30.0, 30.0, 32.1, 32.1, 33.6)

a17 <- c(16, 33.6, 29.7, 31.5, 29.4, 29.4, 27.9, 29.1, 30.0, 30.0, 32.1, 32.1, 33.9)

a18 <- c(17, 33.9, 29.7, 31.5, 29.4, 29.1, 27.9, 28.8, 29.7, 30.0, 32.1, 32.4, 33.9)

a19 <- c(18, 33.9, 29.7, 31.5, 29.1, 29.1, 27.6, 28.8, 29.7, 30.0, 32.4, 32.4, 34.2)

a20 <- c(19, 34.2, 30.0, 31.5, 29.1, 28.8, 27.6, 28.5, 29.7, 30.0, 32.4, 32.7, 34.2)

a21 <- c(20, 34.2, 30.0, 31.5, 29.1, 28.8, 27.3, 28.5, 29.7, 30.0, 32.4, 32.7, 34.5)

a22 <- c(21, 34.5, 30.0, 31.5, 29.1, 28.6, 27.3, 28.2, 29.7, 30.0, 32.4, 32.7, 34.5)

a23 <- c(22, 34.5, 30.0, 31.5, 29.1, 28.5, 27.0, 28.2, 29.4, 30.0, 32.7, 33.0, 34.8)

a24 <- c(23, 34.8, 30.3, 31.5, 28.8, 28.5, 26.7, 27.9, 29.4, 30.0, 32.7, 33.0, 35.1)

a25 <- c(24, 35.1, 30.3, 31.5, 28.8, 28.2, 26.7, 27.9, 29.4, 30.0, 32.7, 33.3, 35.1)

a26 <- c(25, 35.1, 30.3, 31.5, 28.8, 28.2, 26.4, 27.9, 29.4, 30.0, 33.0, 33.3, 35.4)

a27 <- c(26, 35.4, 30.6, 31.5, 28.8, 28.2, 26.4, 27.6, 29.1, 30.0, 33.0, 33.6, 35.4)

a28 <- c(27, 35.4, 30.6, 31.5, 28.8, 27.9, 26.1, 27.6, 29.1, 30.0, 33.3, 33.6, 35.7)

a29 <- c(28, 35.7, 30.6, 31.8, 28.5, 27.9, 25.8, 27.3, 29.1, 30.0, 33.3, 33.9, 36.0)

a30 <- c(29, 35.7, 30.9, 31.8, 28.5, 27.6, 25.8, 27.3, 28.8, 30.0, 33.3, 33.9, 36.0)

a31 <- c(30, 36.0, 30.9, 31.8, 28.5, 27.6, 25.5, 27.0, 28.8, 30.0, 33.6, 34.2, 36.3)

a32 <- c(31, 36.3, 30.9, 31.8, 28.5, 27.3, 25.2, 27.0, 28.8, 30.0, 33.6, 34.5, 36.6)

a33 <- c(32, 36.3, 30.9, 31.8, 28.5, 27.3, 25.2, 26.7, 28.5, 30.0, 33.6, 34.5, 36.9)

a34 <- c(33, 36.6, 31.2, 31.8, 28.2, 27.0, 24.9, 26.4, 28.5, 30.0, 33.9, 34.8, 36.9)

a35 <- c(34, 36.6, 31.2, 31.8, 28.2, 27.0, 24.9, 26.4, 28.5, 30.0, 33.9, 34.8, 37.2)

a36 <- c(35, 36.9, 31.2, 31.8, 28.2, 26.7, 24.6, 26.1, 28.2, 30.0, 33.9, 35.1, 37.5)

a37 <- c(36, 37.2, 31.5, 31.8, 28.2, 26.7, 24.3, 25.8, 28.2, 30.0, 34.2, 35.4, 37.6)
```

```
a38 <- c(37, 37.5, 31.5, 31.8, 28.2, 26.4, 24.0, 25.5, 27.9, 30.0, 34.2, 35.7, 38.1)

a39 <- c(38, 37.5, 31.5, 32.1, 27.9, 26.1, 24.0, 25.5, 27.9, 30.0, 34.2, 35.7, 38.1)

a40 <- c(39, 37.8, 31.8, 32.1, 27.9, 26.1, 23.7, 25.2, 27.9, 30.0, 34.5, 36.0, 38.4)

a41 <- c(40, 38.1, 31.8, 32.1, 27.9, 25.8, 23.4, 25.2, 27.6, 30.0, 34.5, 36.0, 38.7)

a42 <- c(41, 38.1, 32.1, 32.1, 27.9, 25.8, 23.1, 24.9, 27.6, 30.0, 34.5, 36.3, 39.0)

a43 <- c(42, 38.4, 32.1, 32.1, 27.6, 25.5, 22.8, 24.6, 27.6, 30.0, 34.8, 36.6, 39.3)

a44 <- c(42, 38.7, 32.4, 32.1, 27.6, 25.2, 22.5, 24.6, 27.3, 30.0, 34.8, 36.6, 39.6)

a45 <- c(44, 39.0, 32.4, 32.1, 27.6, 24.9, 22.2, 24.3, 27.3, 29.7, 34.8, 36.9, 39.9)

a46 <- c(45, 39.3, 32.7, 32.1, 27.6, 24.9, 21.9, 24.0, 27.3, 29.7, 35.1, 37.2, 40.2)

a47 <- c(46, 39.6, 32.7, 32.1, 27.3, 24.6, 21.6, 23.7, 27.0, 29.7, 35.1, 37.5, 40.5)

a48 <- c(47, 39.9, 33.0, 32.1, 27.3, 24.3, 21.3, 23.4, 27.0, 29.7, 35.1, 37.8, 40.8)

a49 <- c(48, 40.2, 33.0, 32.4, 27.0, 24.0, 21.0, 22.8, 26.7, 29.7, 35.4, 38.1, 41.1)

a50 <- c(49, 40.5, 33.3, 32.4, 27.0, 23.7, 20.7, 22.5, 26.7, 29.7, 35.4, 38.4, 41.7)

a51 <- c(50, 41.1, 33.6, 32.4, 26.7, 23.1, 20.1, 22.2, 26.4, 29.7, 35.7, 38.7, 42.3)

b1 <- c(0, 31.2, 28.2, 31.2, 30.3, 31.2, 30.3, 31.2, 31.2, 30.3, 31.2, 30.3, 31.2)

b2 <- c(1, 31.2, 28.2, 31.2, 30.3, 31.2, 30.3, 31.2, 31.2, 30.3, 31.2, 30.3, 31.2)

b3 <- c(2, 31.2, 28.2, 31.2, 30.3, 31.5, 30.6, 31.2, 31.2, 30.3, 31.2, 30.0, 30.9)

b4 <- c(3, 30.9, 28.2, 30.9, 30.3, 31.5, 30.6, 31.2, 31.2, 30.3, 31.2, 30.0, 30.9)

b5 <- c(4, 30.9, 27.9, 30.9, 30.6, 31.8, 30.9, 31.5, 31.5, 30.3, 30.9, 30.0, 30.6)

b6 <- c(5, 30.6, 27.9, 30.9, 30.6, 31.8, 30.9, 31.8, 31.5, 30.3, 30.9, 29.7, 30.6)

b7 <- c(6, 30.6, 27.9, 30.9, 30.6, 31.8, 31.2, 31.8, 31.5, 30.3, 30.9, 29.7, 30.3)

b8 <- c(7, 30.3, 27.6, 30.9, 30.6, 32.1, 31.2, 32.1, 31.8, 30.3, 30.9, 29.7, 30.3)

b9 <- c(8, 30.3, 27.6, 30.9, 30.9, 32.1, 31.5, 32.1, 31.8, 30.6, 30.6, 29.4, 30.0)

b10 <- c(9, 30.0, 27.6, 30.9, 30.9, 32.4, 31.5, 32.4, 31.8, 30.6, 30.6, 29.4, 30.0)
```

```
b11 <- c(10, 30.0, 27.3, 30.9, 30.9, 32.4, 31.8, 32.4, 32.1, 30.6, 30.6, 29.4, 29.7)

b12 <- c(11, 29.7, 27.3, 30.9, 30.9, 32.7, 31.8, 32.7, 32.1, 30.6, 30.6, 29.1, 29.7)

b13 <- c(12, 29.7, 27.3, 30.9, 31.2, 32.7, 32.1, 33.0, 32.1, 30.6, 30.3, 29.1, 29.4)

b14 <- c(13, 29.4, 27.3, 30.9, 31.2, 33.0, 32.1, 33.0, 32.4, 30.6, 30.3, 28.8, 29.4)

b15 <- c(14, 29.4, 27.3, 30.9, 31.2, 33.0, 32.4, 33.3, 32.4, 30.6, 30.3, 28.8, 29.1)

b16 <- c(15, 29.1, 27.3, 30.9, 31.2, 33.3, 32.4, 33.6, 32.4, 30.6, 30.3, 28.5, 29.1)

b17 <- c(16, 29.1, 27.3, 30.9, 31.2, 33.3, 32.7, 33.6, 32.7, 30.6, 30.3, 28.5, 28.8)

b18 <- c(17, 28.8, 27.3, 30.9, 31.5, 33.6, 32.7, 33.9, 32.7, 30.6, 30.0, 28.2, 28.8)

b19 <- c(18, 28.8, 27.0, 30.9, 31.5, 33.6, 33.0, 33.9, 33.0, 30.6, 30.0, 28.2, 28.5)

b20 <- c(19, 28.5, 27.0, 30.9, 31.5, 33.9, 33.0, 34.2, 33.0, 30.6, 30.0, 27.9, 28.5)

b21 <- c(20, 28.5, 27.0, 30.9, 31.5, 33.9, 33.3, 34.2, 33.3, 30.6, 30.0, 27.9, 28.2)

b22 <- c(21, 28.2, 27.0, 30.9, 31.5, 33.9, 33.3, 34.5, 33.3, 30.6, 30.0, 27.6, 28.2)

b23 <- c(22, 28.2, 26.7, 30.9, 31.8, 34.2, 33.6, 34.5, 33.3, 30.6, 29.7, 27.6, 27.9)

b24 <- c(23, 27.9, 26.7, 30.9, 31.8, 34.2, 33.9, 34.8, 33.6, 30.6, 29.7, 27.6, 27.6)

b25 <- c(24, 27.9, 26.7, 30.9, 31.8, 34.5, 34.2, 34.8, 33.6, 30.6, 29.7, 27.3, 27.6)

b26 <- c(25, 27.9, 26.7, 30.9, 31.8, 34.5, 34.2, 35.1, 33.6, 30.6, 29.7, 27.3, 27.3)

b27 <- c(26, 27.6, 26.4, 30.9, 32.1, 34.8, 34.5, 35.1, 33.6, 30.6, 29.7, 27.3, 27.3)

b28 <- c(27, 27.6, 26.4, 30.9, 32.1, 34.8, 34.5, 35.4, 33.9, 30.6, 29.7, 27.0, 27.0)

b29 <- c(28, 27.3, 26.4, 30.9, 32.1, 35.1, 34.8, 35.4, 33.9, 30.9, 29.4, 27.0, 27.0)

b30 <- c(29, 27.3, 26.1, 30.9, 32.1, 35.1, 34.8, 35.7, 33.9, 30.9, 29.4, 26.7, 26.7)

b31 <- c(30, 27.0, 26.1, 30.9, 32.4, 35.4, 35.1, 36.0, 34.2, 30.9, 29.4, 26.7, 26.4)

b32 <- c(31, 27.0, 26.1, 30.9, 32.4, 35.4, 35.1, 36.0, 34.2, 30.9, 29.4, 26.4, 26.4)

b33 <- c(32, 26.7, 25.8, 30.9, 32.4, 35.7, 35.4, 36.3, 34.5, 30.9, 29.4, 26.4, 26.1)

b34 <- c(33, 26.4, 25.8, 30.9, 32.7, 35.7, 35.7, 36.3, 34.5, 30.9, 29.1, 26.1, 25.8)
```

```
b35 <- c(34, 26.4, 25.8, 30.9, 32.7, 36.0, 36.0, 36.6, 34.8, 30.9, 29.1, 26.1, 25.8)

b36 <- c(35, 26.1, 25.5, 30.9, 32.7, 36.3, 36.3, 36.9, 34.8, 30.9, 29.1, 25.8, 25.5)

b37 <- c(36, 26.1, 25.5, 30.9, 33.0, 36.3, 36.6, 37.2, 34.8, 30.9, 29.1, 25.8, 25.2)

b38 <- c(37, 25.8, 25.5, 30.9, 33.0, 36.6, 36.9, 37.5, 35.1, 30.9, 29.1, 25.5, 24.9)

b39 <- c(38, 25.5, 25.2, 30.9, 33.0, 36.9, 37.2, 37.5, 35.1, 31.2, 28.8, 25.2, 24.9)

b40 <- c(39, 25.5, 25.2, 30.9, 33.3, 36.9, 37.2, 37.8, 35.4, 31.2, 28.8, 25.2, 24.6)

b41 <- c(40, 25.2, 21.9, 30.9, 33.3, 37.2, 37.5, 38.1, 35.4, 31.2, 28.8, 24.9, 24.3)

b42 <- c(41, 24.9, 24.9, 30.9, 33.3, 37.5, 37.8, 38.1, 35.7, 31.2, 28.8, 24.6, 24.0)

b43 <- c(42, 24.6, 24.6, 30.9, 33.6, 37.8, 38.1, 38.4, 35.7, 31.2, 28.5, 24.6, 23.7)

b44 <- c(42, 24.3, 24.6, 30.6, 33.6, 37.8, 38.4, 38.7, 36.0, 31.2, 28.5, 24.3, 23.1)

b45 <- c(44, 24.3, 24.3, 30.6, 33.6, 38.1, 38.7, 39.0, 36.0, 31.2, 28.5, 24.0, 22.8)

b46 <- c(45, 24.0, 24.3, 30.6, 33.9, 38.4, 38.7, 39.3, 36.3, 31.2, 28.2, 23.7, 22.5)

b47 <- c(46, 23.7, 24.0, 30.6, 33.9, 38.7, 39.0, 39.6, 36.6, 31.2, 28.2, 23.7, 22.2)

b48 <- c(47, 23.1, 24.0, 30.6, 34.2, 39.0, 39.6, 39.9, 36.6, 31.5, 27.9, 23.4, 21.9)

b49 <- c(48, 22.8, 23.7, 30.6, 34.2, 39.3, 39.9, 40.2, 36.9, 31.5, 27.9, 23.1, 21.6)

b50 <- c(49, 22.5, 23.7, 30.6, 34.5, 39.6, 40.2, 40.5, 37.2, 31.5, 27.6, 22.8, 21.3)

b51 <- c(50, 22.2, 23.4, 30.6, 34.5, 39.9, 40.8, 41.1, 37.5, 31.8, 27.6, 22.8, 21.0)

N <- data.frame(b1,b2,b3,b4,b5,b6,b7,b8,b9,b10,b11,b12,b13,b14,b15,b16,b17,b18,b19,b20,
        b21,b22,b23,b24,b25,b26,b27,b28,b29,b30,b31,b32,b33,b34,b35,b36,b37,
        b38,b39,b40,b41,b42,b43,b44,b45,b46,b47,b48,b49,b50,b51)

S <- data.frame(a1,a2,a3,a4,a5,a6,a7,a8,a9,a10,a11,a12,a13,a14,a15,a16,a17,a18,a19,a20,
        a21,a22,a23,a24,a25,a26,a27,a28,a29,a30,a31,a32,a33,a34,a35,a36,a37,
        a38,a39,a40,a41,a42,a43,a44,a45,a46,a47,a48,a49,a50,a51)

a <- ceiling(lat)
```

```
b <- floor(lat)

ab <- lat - b

ba <- a - lat

if(hem == "S"){

  s1<- S[a]*ab

  s2 <- S[b]*ba

  s3 <- s1 + s2

  R <- s3[2:13,]

}else if(hem == "N"){

  n1<- N[a]*ab

  n2 <- N[b]*ba

  n3 <- n1 + n2

  R <- n3[2:13,]

}else{

  R <- "Wrong syntax"

}

return(R)

}
```

Appendix D.

Code for creating a function to calculate groundwater recharge using as input: a monthly precipitation and temperature shapefile, latitude, hemisphere, runoff and field capacity.

```
setwd("C:/Portoviejo/base") ##working directory where input information is lacated.

library(sf)

library(dplyr)

library(tidyr)
```

```
rm(list = ls())

for (i in 11:70){

w <- paste("20",i,"-u.shp",sep = "")  ##patterns of shapefiles that contain precipitation,

 ### temperature, field capacity and runoff spatial data for each year

p <- st_read(w)

e1 <- p%>%

  mutate(zone = c(1:nrow(p)))  ##create an ID_zone for each row

e <- as.data.frame(e1)  ##transform sf to dataframe

t <- e%>%  ##create a temperature dataframe selecting the corresponding columns

  select(zone, coeff, FC,"Janua_temp","Febru_temp","March_temp","April_temp","May_temp",

"June_temp","July_temp","Augus_temp","Septe_temp","Octob_temp","Novem_temp","Decem_t
emp")

p <- e%>% ##create a precipitation dataframe selecting the corresponding columns

  select(zone,coeff, FC,"Janua_prec","Febru_prec","March_prec","April_prec","May_prec",
"June_prec","July_prec","Augus_prec","Septe_prec","Octob_prec","Novem_prec","Decem_prec")

colnames(p) <- c("zone","coeff","FC","January","February","March","April","May","June","July",

            "August","September","Octuber","November","December") #change names for
precipitation data frame

p <- p%>%

 gather("month","prec",4:15)

colnames(t) <- c("zone","coeff","FC","January","February","March","April","May","June","July",

            "August","September","Octuber","November","December") #change names for
temperature data frame

t <- t%>%

  gather("month","temp",4:15)

data <- inner_join(p,t)%>%
```

```
 group_by(zone)%>%
 filter(is.na(prec) == FALSE & is.na(temp) == FALSE & temp > 0 & is.na(coeff) == FALSE & prec >= 0
)
##filter locations that don't have precipitation, temperature, or runoff data.
source("latitude.R") #call latitude function
months <- c("January","February","March","April","May","June","July",
        "August","September","Octuber","November","December")
MPMDS <- latitude(1.05 ,"S") ## run latitude function (using as input latitude degrees and S as
south ##hemisphere) to know hours of solar radiation


ET <- data%>% ##chunk to obtain potential evapotranspiration for each zone.
 group_by(zone)%>%
 mutate(Hm = ifelse(temp > 0, ((0.2*temp)^1.514),0))%>%
 mutate(Ha = sum(Hm))%>%
 mutate(a = (6.75*(10^(-7))*Ha^3) - (7.71*(10^(-5))*Ha^2) + 0.01792*Ha + 0.49239)%>%
 mutate(UPET = ifelse(temp <= 0, 0,
                ifelse(temp >= 27, -0.015*(temp^2) + 1.093*temp - 14.208 ,
0.53*((10*temp/Ha)^a))))
ETF <- ET%>%  #add solar radiation hours columns to ET dataframe
 select(-Ha,-Hm,-a)%>%
 mutate(DS = ifelse(month == months[1], MPMDS [1],
          ifelse(month == months[2], MPMDS [2],
          ifelse(month == months[3], MPMDS [3],
          ifelse(month == months[4], MPMDS [4],
          ifelse(month == months[5], MPMDS [5],
```

```
          ifelse(month == months[6], MPMDS [6],
          ifelse(month == months[7], MPMDS [7],
          ifelse(month == months[8], MPMDS [8],
          ifelse(month == months[9], MPMDS [9],
          ifelse(month == months[10], MPMDS [10],
          ifelse(month == months[11], MPMDS [11],MPMDS[12])))))))))))%>%
  mutate(ET = DS*UPET)
rm(data,e,ET,t)
data <- ETF%>% ##obtain surface runoff, water retained into the soil and
  filter(coeff != "na" )%>%  ## water retained into soil-less potential evaporation.
  mutate(SR = as.numeric(prec)*as.numeric(coeff))%>% ##obtain surface runoff
  mutate(INF = as.numeric(prec) - as.numeric(SR))%>%
  mutate(IN_E = as.numeric(INF) - as.numeric(ET))%>%
  group_by(zone)%>%
  mutate(AWL = 0)
d <- arrange(data,zone)
n_m <- 12
n <- length(d$zone)/n_m
for (i in 1:n){  ##loop to obtain accumulated water loss
  k = (n_m*i)- 11
  for (j in 1:n_m){
    if(j == 1 & d$IN_E[k] <= 0){
      d$AWL[k] = d$IN_E[k]
    } else if(j == 1 & d$IN_E[k] > 0){
```

```
    d$AWL[k] = 0
   } else if(d$IN_E[k + j - 1] < 0){
    d$AWL[k+j-1] = d$IN_E[k+j-1] + d$AWL[k+j-2]
   } else{
    d$AWL[k+j-1] = 0
   }
  }
}
d <- d%>%  ## adding field capacity data
  filter(FC > 0)%>%
  mutate(b = 0.455/FC)
n <- length(d$zone)/n_m
for (i in 1:n){ ## add monthly field capacity
  k = (n_m*i)-11
  m <- d$FC[k]
  for (j in 1:n_m){
   if(j == 1 & d$IN_E[k] < 0){
    d$FC[k] <- d$FC[k]*(10^(d$b[k]*d$IN_E[k]))
   } else if(j == 1 & d$IN_E[k] >= 0){
      d$FC[k] <- d$FC[k]
   } else if(j > 1 & d$IN_E[k +j -1] < 0){
      d$FC[k + j - 1] <- d$FC[k + j - 2]*(10^(d$b[k]*d$IN_E[k + j - 1]))
   } else if(j > 1 & d$IN_E[k + j -1] > 0 & d$FC[k + j - 2] +  d$IN_E[k + j -1] <= m ){
      d$FC[k + j - 1] <- d$FC[k + j - 2] +  d$IN_E[k + j -1]
```

```
    } else{
      d$FC[k + j - 1] <- m
    }
  }
}
d <- d%>%
  mutate(FCC = 0)%>%
  select(-DS,-UPET,-b)
for (i in 1:n){  ##adding field capacity changes
  k = (n_m*i)-11
  for (j in 2:n_m){
    d$FCC[k + j - 1] <- d$FC[k + j -1] - d$FC[k + j -2]
  }
}
d <- d%>% ##add water deficit, actual evapotranspiration and percolation columns.
  mutate(WD = ifelse(IN_E <= 0, FCC - IN_E,0))%>%
  mutate(AET = ET - WD)%>%
  mutate(P = ifelse(IN_E >= 0,IN_E - FCC,0))
d
rm(ETF,p,pt,r,rt)
s <- d%>% ##select percolation column
  select(month,P,zone)%>%
  spread(month,P)%>%
  mutate(total = sum(c(April, August, December, February, January, July,  June, March,  May,
November, Octuber, September)))
```

```
e1 <- select(e1, zone)

s2 <- inner_join(e1,s) ##join dataframe to shapefile.

nm <- paste("recharge-",w,sep = "")

st_write(s2,nm)  ##save groundwater recharge dataframe.

}
```